Review

Characterisation of dry powder inhaler formulations using atomic force microscopy

Cordula Weiss*, Peter McLoughlin, Helen Cathcart

Pharmaceutical and Molecular Biotechnology Research Centre (PMBRC), Waterford Institute of Technology, Cork Road, Waterford, Ireland

ABSTRACT

Inhalation formulations are a popular way of treating the symptoms of respiratory diseases. The active pharmaceutical ingredient (API) is delivered directly to the site of action within the deep lung using an inhalation device such as the dry powder inhaler (DPI).

The performance of the formulation and the efficiency of the treatment depend on a number of factors including the forces acting between the components. In DPI formulations these forces are dominated by interparticulate interactions. Research has shown that adhesive and cohesive forces depend on a number of particulate properties such as size, surface roughness, crystallinity, surface energetics and combinations of these. With traditional methods the impact of particulate properties on interparticulate forces could be evaluated by examining the bulk properties. Atomic force microscopy (AFM), however, enables the determination of local surface characteristics and the direct measurement of interparticulate forces using the colloidal probe technique. AFM is considered extremely useful for evaluating the surface topography of a substrate (an API or carrier particle) and even allows the identification of crystal faces, defects and polymorphs from high-resolution images. Additionally, information is given about local mechanical properties of the particles and changes in surface composition and energetics. The assessment of attractive forces between two bodies is possible by using colloidal probe AFM.

This review article summarises the application of AFM in DPI formulations while specifically focussing on the colloidal probe technique and the evaluation of interparticulate forces.

© 2015 Elsevier B.V. All rights reserved.

Contents

1. Introduction

In recent years, atomic force microscopy (AFM) has become one of the most significant tools in surface chemistry with applications ranging from simple topographical imaging to force measurements, including tailor-made colloidal probe measurements, and also meeting specific requirements such as the evaluation of electric forces or magnetic fields.

AFM based research has been found to be particularly beneficial in the field of pharmaceutics, especially in the area of inhalation formulations. Relevant applications will be discussed in this article while focussing on dry powder inhaler (DPI) formulations. Issues regarding such experiments are discussed and an overview of common approaches is given. Additionally, a brief summary of adhesion theories provides a better understanding of the forces dominating DPI formulations and the challenges AFM users have to overcome.

2. Pulmonary drug delivery

Respiratory disorders such as asthma and chronic obstructive pulmonary disease (COPD) are usually treated by direct pulmonary delivery of drug formulations via inhalation (Global Initiative for Asthma, 2014). Owing to the rapid onset of action, the circumvention of the first pass metabolism and a generally lower risk of side effects, inhalation formulations are generally considered superior to conventional oral dose alternatives (Hoppentocht et al., 2014; Patton and Byron, 2007; Sung et al., 2007; Wang et al., 2014). Delivery relies on nebulisers, soft-mist inhalers (SMI), metered dose inhalers (MDI) or dry powder inhalers (DPI), with the latter providing a convenient way of delivering the drug with unique advantages such as easy handling and relatively high patient compliance (Dalby et al., 2004; Hoppentocht et al., 2014; Labiris and Dolovich, 2003a,b; Patton and Byron, 2007; Sung et al., 2007; Wang et al., 2014). In terms of shelf life and drug stability, DPI formulations also benefit from being stored in the solid state which makes the active pharmaceutical ingredient (API) less susceptible to degradation and therefore superior to MDI suspensions (Zeng et al., 2000).

Efficient drug delivery is controlled, first and foremost, by the properties of the formulation. In order to reach the targeted sites in the respiratory tract, the API needs to penetrate the deep lung (Cui et al., 2014). Upon inhalation, the drug particles are subject to different deposition mechanisms—impaction, sedimentation and diffusion—depending on their size (Heyder, 2004; Zeng et al., 2000). Impaction leads to particles with aerodynamic diameters above 5 μm remaining in the oropharynx. APIs with aerodynamic diameters below 5 μm deposit in the smaller airways, including bronchi and bronchioles, where sedimentation by gravitational forces is the main deposition mechanism. A particle's settling velocity correlates directly with the square of the particle diameter (Frijlink and De Boer, 2004), assuming an ideally spherical shape. Therefore, sedimentation depends critically on particle size. Frijlink and De Boer (2004) found particles below 1 μm to be unsuitable for sedimentation. Most particles below this diameter are exhaled while small percentages are drawn into the deepest regions of the lung, the alveoli, where the particles deposit due to diffusion.

The key factor for drug deposition is the aerodynamic diameter of the drug particles (Eq. (1)). The aerodynamic diameter, D_{ae}, depends on the particulate density, ρ_p, the geometric diameter of the particle, D_g, and its geometry, expressed by the dynamic shape factor, χ, which is 1.00 for an ideal sphere but increases with irregularities. D_{ae} represents the diameter of a sphere with a standard density, ρ_o, of 1000 kg m^{-3} and the same terminal velocity as the irregular particle (Wang et al., 2014) (Eq. (1)):

$$D_{as} = D_g \sqrt{\frac{\rho_p}{\rho_o \chi}} \tag{1}$$

For optimum efficacy, the particles' aerodynamic diameters should be between 1 μm and 5 μm (Cui et al., 2014). However, other particle and formulation characteristics are critical too. Moisture uptake needs to be known precisely on account of its impact on the effective aerodynamic particle diameters as the particles migrate through the respiratory tract (Heyder, 2004). Dispersion and flow related properties are also crucial for the success of inhalation therapy. For example, flowability affects the mixing and capsule filling performance (Neumann, 1967; Tan and Newton, 1990), and the detachment of the API from the carrier during inhalation (Zeng et al., 2000).

Successful API delivery is influenced by particle shape, size and size distribution, and also by surface morphology (De Boer et al., 2005; Neumann, 1967). If excipients are included in the formulation, carrier particle size and texture also have to be considered. The forces acting both between drug particles and between drug and excipient particles are of high importance: they have to be strong enough to allow for easy formulation preparation and to prevent segregation during transport and storage (Cui et al., 2014). At the same time, they need to be low enough to ensure dispersion and disaggregation during inhalation (Cui et al., 2014), as only small particles and agglomerates (<5 μm) can penetrate the deep lung and be therapeutically active (Cui et al., 2014; Zeng et al., 2000). The drug load itself also affects formulation performance along with the choice of inhaler device (De Boer et al., 2005) and the patient's individual breathing pattern (Chrystyn and Price, 2009; Heyder, 2004). The relationship between particulate characteristics and their respective effects on formulation performance have been studied and reviewed widely over the years (Adi et al., 2013; Chan, 2008; Chow et al., 2007; Donovan and Smyth, 2010; Guenette et al., 2009; Healy et al., 2014; Zellnitz et al., 2014; Zeng et al., 2000; Zhang et al., 2011).

3. Atomic force microscopy (AFM)

To assess the particulate characteristics of a dry powder formulation, specifically adapted methods are often necessary. This is particularly true for surface analyses, e.g. the evaluation of surface morphology, surface rugosity or surface energetics (Wu et al., 2010) and for determining the interparticulate forces between the API and/or carrier particles (Tsukada et al., 2004). For a number of decades, one technique in particular has proven to be extremely valuable for measuring such forces: atomic force microscopy (AFM). The range of AFM-based applications is summarised in Table 1.

AFM is an advanced technique for surface characterisation studies (Wu et al., 2010). In contrast to conventional optical or

Table 1
Application of AFM in API particle and formulation characterisation.

AFM mode	Output	Use in particle/formulation characterisation
Tapping (intermittent) or contact mode	Topographical mapping	Particle surface morphology (Götzinger and Peukert, 2003; Hooton et al., 2006a; Packhaeuser et al., 2009; Ward et al., 2005)
	Phase imaging	Particle surface roughness (Donovan and Smyth, 2010; Hooton et al., 2006a; Kaialy and Nokhodchi, 2013b)
		Degradation during storage or processing (Begat et al., 2003)
		Crystal growth (Durbin and Carlson, 1992; Price and Young, 2004)
		Crystallinity (Begat et al., 2003; Ward et al., 2005)
		Polymorphism (Danesh et al., 2000; Hooton et al., 2006a)
		3D imaging of the particle (Hooton et al., 2006a)
Nanoindentation	Elastic modulus (local)	Elasticity (Davies et al., 2005; Perkins et al., 2009, 2007)
	Deformation (local)	Hardness (Masterson and Cao, 2008; Perkins et al., 2009)
		Degradation during storage or processing (Perkins et al., 2009)
Force distance measurements	Elastic modulus	Elasticity (Davies et al., 2005; Perkins et al., 2009, 2007)
	Deformation	Hardness (Masterson and Cao, 2008; Perkins et al., 2009)
	Adhesion	Degradation during storage or processing (Perkins et al., 2009)
		Crystallinity (Perkins et al., 2007)
		Particle surface energetics (Davies et al., 2005; Perkins et al., 2009)
		Chemical surface properties (Hooton et al., 2004)
		Correlation of surface specific properties (Perkins et al., 2007; Ward et al., 2005)
Colloidal probe AFM	Adhesion	Physical interaction between materials (Beach et al., 2002; Hooton et al., 2004; Rogueda et al., 2011)
		Chemical interaction between materials (Hooton et al., 2004; Islam et al., 2014; Rogueda et al., 2011)
		Cohesive adhesive balance (Begat et al., 2004a; Jones et al., 2008a,b)
		Particle surface energetics (Hooton et al., 2006a)
		Electrostatic surface properties (Götzinger and Peukert, 2003; Kwek et al., 2011)
		Triboelectric charging (Kwek et al., 2011)
		Surface polarity (Kwek et al., 2011)

electron microscopy, AFM relies on the physical interaction between a probe with a sharp tip and a surface. Three-dimensional height images can be recorded with resolutions within the atomic range (Binnig et al., 1987; Eaton and West, 2010; Giessibl, 2005). At the same time, information about the composition of the surface can be collected (Eaton and West, 2010). By considering and combining all results a thorough understanding of the nature of the sample surface is obtained.

To analyse the surface of a sample, it is fixed onto a motorised stage (Fig. 1). With the help of an optical microscope and a live camera, the substrate is positioned accurately under the probe which itself is fastened onto the scan head. The probe consists of a sharp tip at the free end of a cantilever attached to a chip. The most common materials are silicon (Si) and silicon nitride (Si_3N_4). Piezoelectric elements (made of a material that changes it dimension in response to an applied voltage), either included in the scan head or the AFM stage, ensure precise motion in the

nanoscale. As the probe scans across the sample surface, a laser beam is directed onto the cantilever surface. Upon meeting resistances on the specimen surface the cantilever twists and bends, causing the beam to reflect at different angles. A four-quadrant photodiode captures the light from the reflected laser beam, thus recording the cantilever deflection. The signal from the photodiode is then evaluated by the feedback controller in order to maintain a certain force between tip and sample. By comparing the registered values with those set initially, the feedback control causes the voltage applied to the piezo element to adjust the z-piezo expansion. It is thus possible to control the force exerted onto the sample or to maintain a certain distance between tip and specimen surface. If, for example, the registered force is stronger than it should be, the piezoelectric transducer moves the tip away from the specimen surface and vice versa. Since the voltage applied to the z-piezo changes in accordance with the topography of the
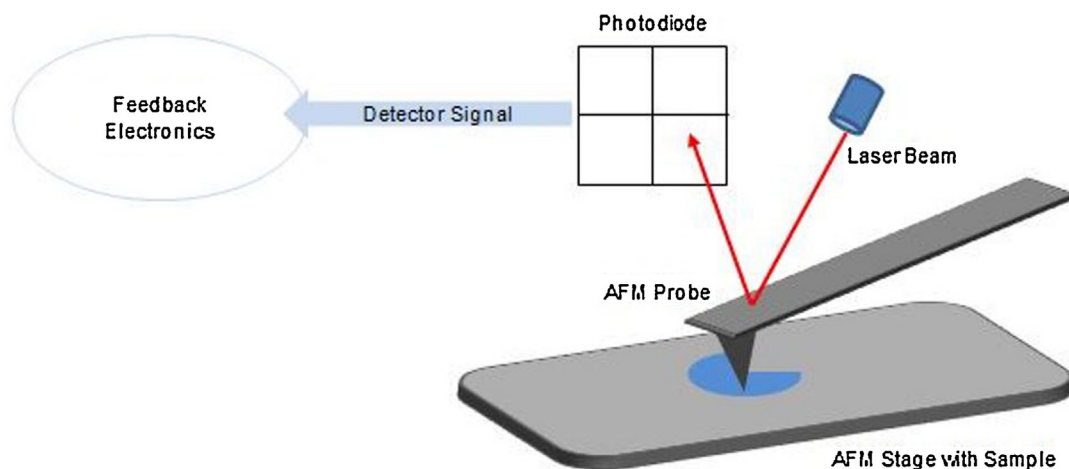

Fig. 1. Schematic overview of AFM measurements. The sample is scanned by an AFM probe onto which a laser beam is directed and reflected onto a four-quadrant photodiode. The signal from the photodiode is then evaluated by the feedback controller. Piezoelectric elements are included in the scan head or the AFM stage to ensure precise motion in the nanoscale.

sample surface, a map of the surface topography is constructed from the corrective factors or error signals (Eaton and West, 2010).

The principle of generating height images by physically detecting the topography of a surface can be traced back almost 90 years (Eaton and West, 2010). In 1929, Schmalz introduced an instrument, the Stylus Profiler, which consisted of a sharp tip on a cantilever (Schmaltz, 1929) and relied on similarly designed optical levers as today's AFM (Eaton and West, 2010).

In 1972, Young et al. introduced the Topografiner (Young et al., 1972) and used it to create an image of a surface by monitoring the electron field emission current between a metal probe and a surface (instead of physical contact). This was the first time piezoelectric elements were employed to move a probe in all directions. The same concept is still used today to scan an AFM probe over a surface (Eaton and West, 2010).

Late in December 1978, Binnig and Rohrer filed a patent application (Binnig and Rohrer, 1981) for the invention of the scanning tunnelling microscope (STM). The STM was based on the Topografiner but produced images of a higher resolution by recording the more distance-sensitive tunnelling current instead of the field emission current (Eaton and West, 2010). For their invention, Binnig and Rohrer received the Nobel Prize for physics in 1986 (Deutsches Patent-und Markenamt, 2014). The first AFM, as described by Binnig, Quate and Gerber (Binnig et al., 1986), differed from the STM only through the use of a diamond on a gold cantilever instead of a probe made of wire. Further improvements led to the introduction of standardised ready-to-use Si- and Si_3N_4-probes (Eaton and West, 2010).

Today, AFM images can be obtained in various ways depending on the sample surface and the desired results. There are basically three different AFM modes used for the generation of height maps: contact, non-contact and intermittent contact mode. AFM also offers a number of more specific modes of operation, such as force spectroscopy and mechanical property mapping; electric, lateral and magnetic force spectroscopy; tunnelling atomic force microscopy and thermal analysis, to name just a few (Eaton and West, 2010).

3.1. Topographical imaging

Topographical imaging is an excellent tool for visualising small particles. AFM measurements are not hampered by many of the issues associated with scanning electron microscopy (SEM) (Lamprou and Smith, 2014). Samples are not prone to charging and do not require any specific preparatory steps such as carbon or gold coating. Subtle features which are likely to be lost in SEM are correctly displayed in AFM images. The careful acquisition of an AFM height map therefore gives information about the sample surface morphology, along with quantitative measurements such as length, depth, volume and surface area (Eaton and West, 2010; Lamprou and Smith, 2014).

In the early 1990s, topographical imaging was first used to follow the growth of crystals. Examples such as the investigation of the stepwise growth of lysozyme crystals by Durbin and Carlson (1992) and the observation of a layer wise growth mechanism of hydroxyapatite crystals by Onuma et al. (1995) are summarised by Lamprou and Smith (2014). AFM was shown to be a useful tool for identifying specific crystal faces: Thompson et al. (2004) scanned the (0 0 1) faces of aspirin and demonstrated that structural transformations in crystalline materials can be observed under the AFM.

The high resolution of topographical images (Eaton and West, 2010) not only allows for differentiation between crystal faces, but also the investigation of surface structures and textures at an atomic level. Thus, AFM can be used both to differentiate between highly-ordered crystalline regions and amorphous areas and to

assess different polymorphic forms. Different polymorphs generally have different physicochemical properties such as melting point or water content. In pharmaceutical applications, knowledge of the respective polymorphic form is crucial as it affects solubility, dissolution, stability and shelf life and the performance of the drug. Insulin, for example, was studied by Yip and Ward (1996); the group imaged the crystal faces of different polymorphs, distinguished single steps on these surfaces and even followed the growth process. Similarly, Danesh et al. (2000) investigated the two polymorphic forms of cimetidine and Hooton et al. (2006a) distinguished between four polymorphic forms of sulfathiazole. Of course, X-ray diffraction (XRD) also enables the determination of crystal unit cells and the distinction of polymorphs. The main advantage of AFM over XRD, however, lies in its ability to acquire high-resolution images of crystalline defects such as steps, terraces or impurities; to monitor the process of crystal growth; and to identify amorphous regions on predominantly crystalline surfaces.

The ability to identify amorphous regions of a surface makes AFM suitable for the evaluation of the surface stability of different materials. This is particularly useful for analysing milled powders, e.g. milled salbutamol sulphate particles (Begat et al., 2003). When a material is subjected to a high-energy milling process, amorphous regions are created which then affect the material's stability. Begat et al. (2003) compared the structure of crystals before and after micronisation using cross-sectional AFM surface analysis (scanning cross sections of processed and unprocessed crystals) and observed the emergence of additional amorphous regions. Increasing the milling times lowered the ratio of crystalline to amorphous areas (Begat et al., 2003). This agreed with moisture sorption data which showed a higher degree of moisture uptake by milled particles, indicating an increasing amount of amorphous material on the surface. These results support the theory that high energy processing leads to an increase in surface energy and confirm the applicability of AFM regarding the identification of surface irregularities at the nanoscale and the investigation of possible surface instabilities.

Carrier based formulations also need to be optimised in terms of their excipient properties. To date, lactose tends to be the carrier material of choice—but researchers (Hooton et al., 2006b; Kaialy et al., 2011, 2010; Kaialy and Nokhodchi, 2012, 2013a,b; Packhaeuser et al., 2009) are working towards the use of sugar based substitutes such as mannitol, raffinose, trehalose, xylitol and cyclodextrin; novel materials such as polymer nano-carriers (Paranjpe and Müller-Goymann, 2014); and the development of carrier free formulations (Healy et al., 2014). AFM has been used to evaluate the morphology of freeze-dried mannitol, a promising carrier species (Packhaeuser et al., 2009). In carrier based blends, the carrier surface morphology and rugosity play critical roles in terms of interparticulate forces. Both properties affect the adhesive interactions and therefore the performance of the formulation. Numerous groups (Bosquillon et al., 2001; Donovan and Smyth, 2010; Flament et al., 2004; Heng et al., 2000; Jones and Price, 2006; Kinnunen et al., 2014; Ooi et al., 2011; Young et al., 2009; Zellnitz et al., 2013, 2014) investigated the correlation between excipient particle size, surface roughness and formulation performance with the aim of optimising these properties. Formulation performance was related to particle size and roughness of a budesonide–lactose formulation by Donovan and Smyth (2010); particle roughness and adhesion of a terbutaline sulphate–lactose formulation by Flament et al. (2004); and to the percentage of carrier surface coverage in a model salbutamol sulphate formulation by Zellnitz et al. (2014). Ferrari et al. (2004) looked at the effect of wet-smoothing on the rugosity of lactose carrier particles. A sequence of alternate steps of wetting and drying in a high-shear mixer smoothed the particle edges and resulted in a less rough surface. The application of water sprayed from an ultrasound nebuliser also improved the particle

surface smoothness and the flowability of the formulation (Genina et al., 2009).

In other studies, lactose was either recrystallised from different solutions (Kaialy et al., 2011) or spray-dried and recrystallised in a humid environment (Price and Young, 2004). The growth process was followed using AFM topographical imaging in combination with conventional optical microscopy. Price and Young (2004) were able to distinguish between primary and secondary nucleation processes occurring at different levels of relative humidity (RH), and to show that low RH resulted in the formation of unstable amorphous lactose particles. Differences in surface structure and roughness of mannitol, a promising substitute for lactose, were also assessed by AFM. Compared to commercial and spray-dried mannitol, the freeze-dried particles (Kaialy and Nokhodchi, 2013a) showed a lower roughness which might account for the improved aerosolisation performance (Kaialy and Nokhodchi, 2013a; Zeng et al., 2000). At the same time, the fine particle fraction (FPF) (the fraction of particles in the emitted dose with $D_{ae} \leq 5 \, \mu m$ (Cui et al., 2014)) was comparatively high. Similarly, the treatment of mannitol particles in a saturated mannitol solution also decreased surface roughness and yielded high FPFs (Kaialy and Nokhodchi, 2013b). These findings suggest that for mannitol particles, surface roughness is the property with the most significant effect on flowability, aerosolisation and FPF (Kaialy and Nokhodchi, 2012, 2013b); while shape and size have a lower impact.

Being well aware of the importance of surface roughness, many groups use AFM topographical imaging to evaluate the roughness of API and excipient particles before continuing with the main aspects of their studies. Researchers rely on the root mean square (RMS) roughness (Berard et al., 2002a,b; Bouhroum et al., 2010; Hickey et al., 2007; Hooton et al., 2006a,b; Traini et al., 2006; Young et al., 2009), and sometimes also include the arithmetic average (Begat et al., 2004a; Kinnunen et al., 2014).

3.2. Mechanical properties

AFM is a valuable tool for studying the mechanical properties of API and excipient particles. Properties such as elasticity, hardness and deformation must all be considered as the interparticulate interactions within a formulation are affected by these characteristics. While conventional stress-strain testing, e.g. four-point beam bending (Bassam et al., 1990) and nanoindentation (Egart et al., 2014), provide good results for bulk mechanical properties, AFM-based measurements have been employed repeatedly to evaluate the local properties of single particles. Force distance curves (force curves) are acquired to obtain information about mechanical properties and interparticulate interactions (Fig. 2) (Pittenger et al., 2010). Initially, the movement of the z-piezo and

the deflection of the cantilever are recorded over time. Highly developed software programmes allow the conversion of the measured deflection into force (Fig. 2a and b) (Pittenger et al., 2010). For interpretation purposes, the force is then plotted against the separation between the tip of the probe and the sample surface which is derived from the position of the z-piezo (Fig. 2c and d) (Pittenger et al., 2010).

The impact of processing on the mechanical properties of budesonide and ipratropium bromide was determined via AFM by Kubavat et al. (2012) and Shur et al. (2012), respectively. Similarly, Davies et al. (2005) investigated the local elastic modulus of budesonide. Masterson and Cao (2008) and James et al. (2008) demonstrated the success of the technique by assessing the elastic moduli of a range of materials: formoterol fumarate, salmeterol xinafoate, salbutamol sulphate, mometasone furoate and salmon calcitonin (Masterson and Cao, 2008) and by evaluating the hardness of drug, lactose and sucrose particles (James et al., 2008).

AFM can be used to determine the Young's modulus of a specific crystal face as demonstrated by Perkins et al. (2007) on a (0 0 1) face of a lactose crystal. The assessment of local elastic moduli at different points of a surface enables the distinction between amorphous and crystalline regions of a substrate in addition to purely topographical characterisation. Ward et al. (2005), for example, successfully combined AFM nanoindentation, topographical mapping and 3-D Raman studies to distinguish crystalline from amorphous areas. Care should be taken, however, with the repeated acquisition of AFM force curves from the same amorphous location as this may lead to pressure induced phase transitions (Perkins et al., 2007).

Another aspect to be investigated is the relation between the hardness/Young's modulus ratio of a particle and its micronisation behaviour. This was first studied by Perkins et al. (2009) who discovered a relationship between the hardness/Young's modulus ratio of carbamazepine polymorphs which were milled for different periods of time, and the resulting particle size reduction and surface energy change.

4. Colloidal probe AFM

Colloidal probe AFM, developed by Butt (1991) and Ducker et al. (1991) in the early 1990s, involves attaching a particle to a tipless cantilever and using the modified probe to investigate the interactions between the attached particle and a substrate (Butt et al., 2005). The method requires careful preparation of the probe. Issues related to the size of the components can be overcome using a micromanipulator and a microscope. However, the user needs to take care to choose a particle without any loosely attached debris on the surface. For accurate measurements, the particle is best

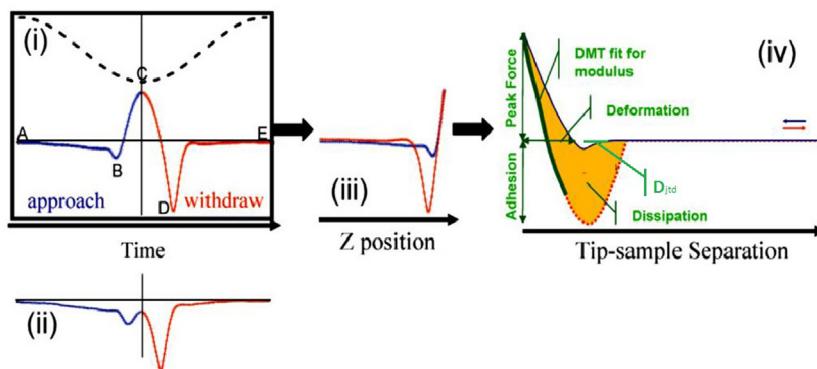**Fig. 2.** Force distance curve acquisition and conversion. (a) Plot of force and z-piezo position as a function of time, including (B) snap-on, (C) peak force, (D) snap-off, (b) plot of force vs. time, (c) force curve consisting of plotting force vs. z-piezo position, (d) plot force vs. separation and information given by the plot. Reprinted with permission from Bruker Nano Surfaces Division, Tucson, AZ, USA.

mounted on the very end of the cantilever in a central position. When attaching the particle, the smallest amount of glue possible should be applied to prevent contamination, minimise excess glue and reduce the impact of the additional mass on the effective spring constant of the cantilever. If the particle is small enough, attractive forces alone might be enough to hold it in place. Once the particle is in position, further modifications can be performed to obtain an ideal surface. These may include ultrasonic cleaning, etching processes or coating. Fig. 3 shows one possible technique for gluing a glass microsphere onto a tipless cantilever. Firstly, all materials (glass microspheres, glue and cantilever) are placed on a suitable surface, e.g. a Si wafer (Fig. 3a and b). A needle is attached to a micromanipulator and all steps are performed under an optical microscope. The needle is dipped slightly into the glue, aligned over the cantilever and then slowly lowered until a minute amount of glue is transferred to the surface of the cantilever (Fig. 3c). With a second needle, a glass microsphere is picked up using capillary forces and placed directly on top of the drop of glue (Fig. 3d). After curing, the prepared AFM probe can be immersed into a solution or dispersion for coating purposes (Fig. 3e and f) using either the micromanipulator or the AFM piezo elements (Islam et al., 2014) to adjust the z-position until the sphere is covered.

Islam et al. (2014) used the latter method to coat silica microspheres with salbutamol sulphate using commercially-available cantilevers with pre-attached silica beads. These commercial cantilevers are less susceptible to damage and contamination and benefit from a lower deviation of the spring constant compared to manually prepared probes which is significant for accurate results. The effective spring constant is affected by both the position and the mass of the attached particle (Ohler, 2007). As the spring constant is one of two factors used to calculate the force acting between the bodies (Eq. (7)), its validity is crucial for correct measurements. Several techniques to assess the effective spring constant have been found, evaluated and refined in the last two decades (Cleveland et al., 1993; Glotzbach et al., 2013; Hutter and Bechhoefer, 1993a; Ohler, 2007; Sader et al., 1995). They are based on a shift in the resonant frequencies before and after modification. Most AFM software packages now allow the automatic determination of the spring constant via thermal tuning which is based on the specific movement of a cantilever upon the application of thermal noise (Serry, 2005). However, common calibration methods (Green et al., 2004) for rectangular cantilevers mainly rely on the techniques developed by Cleveland et al. (1993) or Sader et al. (1999, 1995). The Cleveland method, yielding the spring constant, k_{clv}, (Eq. (2)) uses the resonant frequency, ω, (Eq. (3)) which depends the mass of the particle attached to the free end of the cantilever, M_s, and the effective cantilever mass, M^*, and correlates to the spring constant, k. The resonant frequency before cantilever modification, ω_0, differs from the resonant frequency measured after cantilever modification, ω_1.

$$k_{clv} = 4\pi^2 \frac{M_s}{\omega_1^{-2} + \omega_0^{-2}} \tag{2}$$

$$\omega^2 = \frac{k}{M^* + M_s} \tag{3}$$

Sader et al. (1999, 1995) suggested deriving the spring constant (Eq. (4)) in air, k_{sad}, from the width, b, and length, l, of the cantilever, the unloaded radial resonant frequency, ω_0, the air density, ρ, the quality factor in air, Q_f, and the imaginary component of the hydrodynamic function, $\Gamma_i(\omega_0)$:

$$k_{sad} = 0.1906 b^2 l \omega_0^2 \rho Q_f \Gamma_i(\omega_0) \tag{4}$$

On account of the sphere not being placed exactly at the free end of the cantilever (off-end loading), the actually exerted force differs slightly from the theoretical force. For this reason, the length of the cantilever, l, and the position of the sphere, Δl, need to be included in the calculation of the off-end spring constant, k_{off}, (Eq. (5)) (Glotzbach et al., 2013; Green et al., 2004). In Eq. (5), k represents the previously determined spring constant in accordance with either the Cleveland, k_{clv}, or the Sader method, k_{sad}.

$$k_{off} = k \left(\frac{l}{l - \Delta l} \right)^3 \tag{5}$$

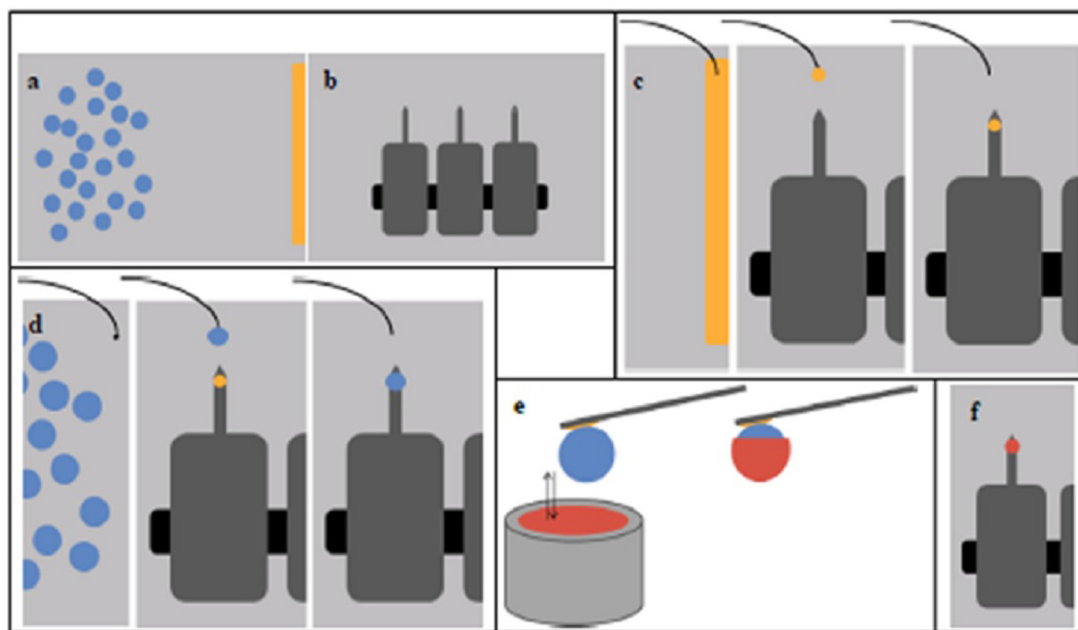**Fig. 3.** Colloidal probe AFM. (a) Preparation of glue and glass microspheres on a silicon wafer, (b) preparation of tipless cantilevers on a silicon wafer, (c) dropping glue onto the free end of a cantilever with a needle, (d) moving glass microsphere to the cantilever with a needle, (e) dipping glass microsphere into a dispersion for coating (optional) and (f) coated glass microsphere glued to the cantilever.

Additionally, the inclination of the cantilever has to be considered when conducting force measurements. The tilt angle, α, can be included in the calculation of the effective spring constant as follows (Eq. (6)) (Benmouna and Johannsmann, 2003; Butt et al., 2005):

$$k_{\text{eff}} = k_{\text{off}} \cos^{-2}(\alpha) \tag{6}$$

Other methods of calculating the spring constant include using fluids with a defined viscosity and measuring the respective drag force on the modified cantilever (Craig and Neto, 2001; Notley et al., 2003) or exposing the cantilever to a gas flow from a microchannel and evaluating the effect exerted on the cantilever's resonant frequency (Parkin and Hähner, 2013, 2014). The unknown spring constant of a cantilever can also be obtained by pressing it against a calibrated reference cantilever (Gates and Reitsma, 2007).

In force spectroscopy measurements, force curves are recorded at various points on the substrate surface. The force curves describe the attractive or repulsive forces between the tip and the sample as the tip approaches the surface and is withdrawn again to its initial position (Fig. 4).

The forces acting between sample surface and tip cause the cantilever to deflect. A laser beam reflected from the cantilever surface captures this movement using a photodiode, allowing the cantilever deflection, x_c, to be calculated. This value is then converted into a force, F, using Hooke's law (Eq. (7)), where k_{eff} is the effective spring constant of the cantilever (Butt et al., 2005).

$$F = -\chi_c k_{\text{eff}} \tag{7}$$

The force is plotted against the tip-sample separation, D, (Eq. (8)) given by the sum of the cantilever deflection, x_c, and the piezo position, x_p (Butt et al., 2005).

$$D = \chi_c + \chi_p \tag{8}$$

Fig. 4 shows that initially no interactions are present between the bodies (A) as the probe approaches the sample. At a certain tip-sample separation, the attractive forces cause the tip to snap to the surface (snap-in, B). However, once the tip has snapped to the surface, the repulsive forces gradually start to grow as the tip continues to approach the surface until they exceed the attractive forces and a net repulsive force is recorded. This continues until a pre-defined peak force is reached (C) whereupon the probe begins to withdraw again. The repulsive forces then decrease (D) until the

attractive forces are dominant, holding the tip on the surface and preventing the probe from being withdrawn further. The tip only breaks away from the sample when the force pulling the cantilever back is larger than the adhesive forces holding the tip on the surface (snap-off, E) and the probe then continues to withdraw to its original position. The force of adhesion can be measured directly from the snap-off force at E.

The force exerted between the tip and the sample surface are a combination of attractive van der Waals (vdW) forces and long range Coulomb forces (Cappella and Dietler, 1999). VdW forces include forces between permanent dipoles (Keesom forces), forces between induced dipoles and permanent dipoles (Debye forces) and dispersion forces or forces between induced dipoles (London forces). Their magnitude depends both on the intermediate medium and on the geometry of the bodies in contact. Snap-in occurs when the attractive vdW forces are large enough to overcome any repulsive forces and the cantilever elastic constant (Cappella and Dietler, 1999).

Assuming ideal conditions, i.e. the absence of both electrostatic and capillary forces, the only forces affecting the adhesion of two bodies are vdW forces, F_{vdw} (Eq. (9)). These generally depend on the separation distance, D, the effective radius, R^*, and the Hamaker constant, A (Israelachvili, 2011; Leite et al., 2012):

$$F_{\text{vdw}} = -\frac{AR^*}{6D^2} \tag{9}$$

R^* represents the effective radius and depends on the radii of sphere A and B (Eq. (10a)):

$$R^* = \frac{R_A R_B}{R_A + R_B} \tag{10a}$$

For the interactions between a sphere, A, and a plane, Eq. (10b) is valid:

$$R^* = R_A \tag{10b}$$

The presence of a liquid film covering each surface also affects the vdW forces and the mere presence of a thin layer of liquid, even if it is no more than a monolayer, changes the adhesive interaction between the bodies considerably. Leite et al. (2012) demonstrated that the film thickness per se has a negligible effect which is taken into account by the Hamaker constant. The Hamaker constant is based on the chemical and physical characteristics of the tip, the
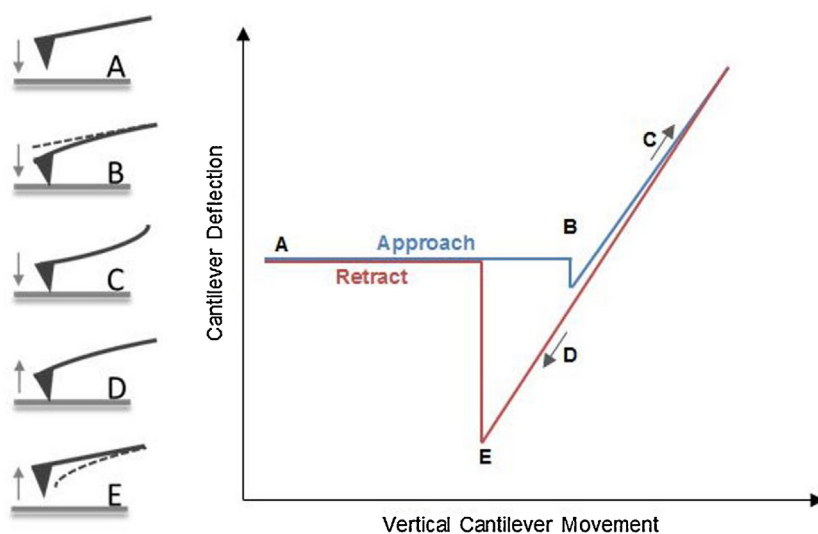
Fig. 4. Cantilever deflection recorded in force distance curve. Cantilever deflection vs. cantilever movement in one approach and withdraw cycle. The cantilever deflection is then converted into force to result in a force curve, showing the point of snap-on, B, and the point of snap-off, E.

sample and the intermediate medium, which includes any adsorbed liquid layers on the surfaces (Fröberg et al., 1999). Geometrical factors, though affecting the vdW forces, are irrelevant to the Hamaker constant (Israelachvili, 2011).

In general, the attractive forces holding the tip on the surface before the snap-off are larger than those causing the snap-in as capillary and meniscus forces along with viscoelastic forces contribute to the overall force of adhesion measured at the snap-off. Chemical bonds between the probe and the substrate may further increase the snap-off force. The adhesive forces depend on probe radius, depth of indentation, elastic or plastic deformation, surface morphology, surface roughness and the actual area of interaction. There is also a significant difference between performing the measurements in air or gaseous atmospheres and in liquid. Thus, both the specific environmental and experimental parameters and the free surface energy of the material have to be considered (Cappella and Dietler, 1999; Leite et al., 2012). A clear distinction between all these factors is impossible without substantial effort (the ideal experiment would require completely smooth and homogeneous surfaces with well-defined properties and strictly controlled experimental settings). Nevertheless, force curves enable the determination of attractive forces between two bodies through the evaluation of the snap-in and snap-off forces (Butt et al., 2005; Cappella and Dietler, 1999).

The energy dissipation (Fig. 2), also referred to as the work of adhesion, corresponds to the difference in the area under the force curve. The work of adhesion, first introduced by Harkins (1928), is often used to indicate the strength of adhesion between two bodies, normalised to the energy of adhesion per unit area.

The presence, and even the thickness, of a liquid film can also be illustrated by AFM, using the jump-to-contact distance. Theoretical calculations (Hutter and Bechhoefer, 1993b) (Eq. (11)) prove the applicability of AFM and show the relationship between the jump-to-contact distance, D_{jtc}, (Fig. 2) at the snap-on and the Hamaker constant, A, the probe tip radius, R_t, and the reduced spring constant, k^*, depending on both sample and cantilever stiffness.

$$D_{jtc} = \sqrt[3]{\frac{AR_t}{3k^*}} \qquad (11)$$

4.1. Adhesion theory

Both cohesive (drug–drug) and adhesive (excipient-drug and container-drug) interactions have a critical effect on the aerosolisation and dispersion of DPI formulations during inhalation. The attractive interaction between each material is determined by many factors including the particles' surface free energy and surface forces, the contact area, the distance between the bodies and the liquid or gaseous medium. The surface forces, referring to the forces present while the two bodies are far apart and separated by a third medium, and the adhesive forces, i.e. the forces acting between the bodies when they are directly in contact with each other, may be equal. Generally, however, they differ by the amount of energy dissipated during the process of the two bodies coming into contact (Bhushan, 2010).

Adhesive forces are crucial for DPI blends consisting of API and carrier particles. They need to be high enough to enable the successful preparation of the formulation, provide stability and prevent segregation during storage (Cui et al., 2014). At the same time, they should not be low enough to not hinder particle disaggregation upon inhalation (Cui et al., 2014).

Force curves acquired by AFM experiments are very well suited to calculate both the forces holding the particles together and the energy needed to separate them. From the snap-off force the work of adhesion can be calculated once the radius is known (Bhushan,

2003). However, all adhesion theories are based on simplifications and assumptions (Leite et al., 2012) and the limitations of the models (summarised below) should be kept in mind when interpreting the data.

4.1.1. Hertzian model

In AFM adhesion measurements, particularly in colloidal probe AFM measurements, the contact area needs to be known in order to obtain reliable results. When two bodies come into contact, the contact area is affected by the deformation of each material. The mechanics of contact between two perfectly elastic, ideally smooth and homogeneous spherical bodies was described by Hertz (1882). Adhesion is not taken into account by this model. Nevertheless, it provides a first estimation of the contact area radius, r_H, as a function of the radius of a sphere, R, the normal force applied to this sphere, F_n, and the reduced Young's modulus, E^*, which depends on the respective materials' characteristics (Eq. (12)):

$$r_H^3 = \frac{RF_n}{E^*} \qquad (12)$$

Further theories modelling contact mechanisms, including adhesion, are built on Hertz's findings.

The area of interaction between an ideally spherical particle and a flat substrate can be calculated in accordance with the adhesion theories developed by Derjaguin, Muller and Toporov (DMT model) (Derjaguin et al., 1975) and Johnson, Kendall and Roberts (JKR model) (Johnson et al., 1971).

4.1.2. Derjaguin–Muller–Todorov (DMT) model

The DMT model (Derjaguin et al., 1975) is used when analysing materials with large elastic moduli. It describes the ideal case of a small sphere, e.g. an AFM probe, being applied to a stiff surface (Leite et al., 2012). Based on the probe radius, R, the normal force, F_n, the reduced Young's modulus, E^*, and the work of adhesion, W_{DMT} (Derjaguin et al., 1975; Dos Santos Ferreira et al., 2010), (Eq. (14)) the contact radius, r_{DMT}, is defined using Eq. (13):

$$r_{DMT}^3 = \frac{R}{E^*}(F_n + 2\pi R W_{DMT}) \qquad (13)$$

where

$$W_{DMT} = -\frac{F_c}{2R} \qquad (14)$$

The DMT model utilises the force of adhesion or critical force, F_c, at the snap-off from an AFM force curve (Leite et al., 2012) and normalises the result through the radius of the probe, R. Depending on the method, the radius either represents that of a spherical particle attached to the cantilever or the tip of a commercial probe.

4.1.3. Johnson–Kendall–Roberts (JKR) model

When larger spherical colloidal probes are used instead of sharp tips, the JKR model (Johnson et al., 1971) is better suited to calculate the contact radius. This model is based on the behaviour of surfaces with higher surface energies and lower elastic moduli; it therefore describes the dependence between a dull probe and a flat surface quite well. The contact radius, r_{JKR}, and the work of adhesion, W_{JKR}, are related to the probe radius, R, the normal force, F_n, and the reduced Young's modulus, E^*, as shown in Eq. (15):

$$r_{JKR}^3 = \frac{R}{E^*}\left[F_n + 3\pi R W_{JKR} + \sqrt{(3\pi R W_{JKR})^2 + 6\pi R F_n W_{JKR}}\right] \qquad (15)$$

The work of adhesion is calculated from the critical force, F_c, and the probe radius, R (Eq. (16)):

$$W_{JKR} = -\frac{2F_c}{3R} \qquad (16)$$

The JKR theory allows for an increased contact area radius when softer materials are in contact and greater deformation occurs (Johnson et al., 1971). In contrast to the DMT model, the theory assumes that two bodies separate when their contact area is 0.63 times the contact area at zero applied force (Leite et al., 2012).

4.1.4. Muller–Yushchenko–Derjaguin (MYD) model

The DMT and the JKR models represent two extreme cases and are valid under different conditions. In reality, neither the DMT nor the JKR model is completely and absolutely correct, but one usually suits better than the other. To evaluate their applicability, Tabor (Tabor, 1977) and Muller, Yushchenko and Derjaguin (Muller et al., 1980) developed the MYD model to calculate the Tabor constant, μ, (Eq. (17)) to select the most appropriate model. The calculation considers the probe radius, R, the work of adhesion, W_{adh} (equal to either W_{DMT} or W_{JKR}), the reduced elastic modulus, E^*, and the equilibrium separation (interatomic distance) of the bodies, D_0 (Dos Santos Ferreira et al., 2010; Leite et al., 2012; Muller et al., 1980).

$$\mu = \left(\frac{16RW_{adh}^2}{9(E^* - 2D_0^3)} \right)^{1/3} \qquad (17)$$

Tabor suggested applying the DMT model if $\mu < 1$ and the JKR model if $\mu > 1$ (Tabor, 1977). Dos Santos Ferreira et al. (2010) set even stricter limits: the DMT model is better suited for $\mu < 0.1$ while the JKR theory applies when $\mu > 5$. Otherwise, the suitability of each model should be considered separately in terms of surface properties such as rigidity or softness and probe radius.

4.1.5. Roughness and deformation

It should be noted that none of the above theories takes the influence of surface roughness into account. All methods are based on an ideally smooth surface even though the impact of morphology and roughness is generally acknowledged and investigated (Beach et al., 2002). Increased surface roughness leads to a decrease in contact area as shown in Fig. 5a. In addition, plastic and elastic deformation caused by pressing the probe into the substrate surface further increases the difficulty of accurately determining the contact area, especially since surface asperities might be crushed or levelled during analysis (Fig. 5b). Sindel and Zimmermann (2001) for example demonstrated the deformation occurring to colloidal lactose probes when pressing them onto a lactose substrate. However, despite investigation, quantifying the impact of surface roughness and surface deformation on the force of adhesion has remained almost impossible (Cline and Dalby, 2002; Louey et al., 2001; Price et al., 2002). The accuracy of the force measurements may therefore be significantly reduced. Rabinovich et al. (2000a,b) have developed a number of promising models which include the impact of nanoscale asperities as well as the irregularity of these asperities themselves.

Cohesive and adhesive forces can be influenced by changing the size and the surface energy of the materials involved. Smaller particles, especially drug particles in the range of 1–5 μm, have a high surface energy and substantial adhesive and cohesive

properties (Zeng et al., 2000). A number of techniques have been developed to evaluate these properties. Contact angle (CA) measurements allow the theoretical determination of the work of adhesion of the bulk material (James et al., 2008). In CA experiments based on the sessile drop method, a liquid, usually water, is dropped onto the sample surface. Depending on the surface energetics and properties of the materials involved, the drop may either spread or maintain its compact form as displayed in Fig. 6.

The contact angle between solid and liquid, θ, is then measured. Young's equation (Eq. (18)) (Young, 1805), relying on the cosine of the contact angle, gives information about the interfacial forces between solid and liquid, γ_{SL}, liquid and vapour, γ_{LV}, and solid and vapour, γ_{SV}.

$$\gamma_{LV} \cos\theta = \gamma_{SV} - \gamma_{SL} \qquad (18)$$

Ultracentrifuges were also used for many years to directly measure adhesion (Götzinger and Peukert, 2003; Lam and Newton, 1991; Podczeck et al., 1994, 1997). In this method, particles adhered to a plane surface of a compressed material are detached by centrifugal forces. The evaluation of the adhesive or cohesive force is based on the number of particles remaining on a certain area of the surface after centrifugation at a defined speed.

However, for the evaluation of forces between single particles, the AFM colloidal probe technique is regarded as the method of choice today (Götzinger and Peukert, 2003). Butt et al. (2005), Cappella and Dietler (1999) and Leite et al. (2012) have published valuable articles regarding the determination of interparticulate forces using the colloidal probe technique.

4.2. Adhesion measurements

A substantial number of groups have used colloidal probe AFM (Fig. 3) to evaluate both the cohesive and adhesive interactions between materials used in drug delivery (Adi et al., 2007; Beilmann et al., 2007; De Boer et al., 2003a,b; Eve et al., 2002; James et al., 2008; Karner et al., 2014; Louey et al., 2001; Price et al., 2002; Sindel and Zimmermann, 2001; Tsukada et al., 2004; Young et al., 2009) and, quite recently, the mechanism of particle detachment (Cui and Sommerfeld, 2015). While three different scenarios describing the process of particle detachment—lift-off, sliding and rolling—are possible, a combination of colloidal probe measurements, simulations and computational modelling identified the rolling mechanism, closely followed by sliding, as the main mechanisms of particle detachment.

Crean et al. (2009) developed a novel AFM-based technique for rheological measurements. The group used colloidal probe AFM to determine the rheology of inter-granular bridges between lactose and polyvinylpyrrolidone particles at different RH.

The impact of particle size on interparticulate forces must be considered when performing colloidal probe experiments as the contact area is strongly influenced by the diameter of the bodies. Two techniques for assessing the true tip radius have been proven to be effective in practice: one relies on SEM imaging (Glotzbach et al., 2013), while the second records the shape of a mounted
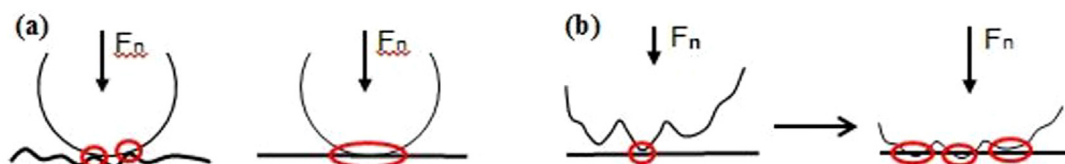

Fig. 5. Influence of surface roughness and particle deformation on contact area. (a) Effect of roughness; the area of interaction is made up of several points of contact if asperities determine the surface and a rough surface may also decrease the overall contact area; (b) effect of deformation on contact area; the area of interaction not only increases when a larger normal force is applied but may also consist of a larger number of points of contact.
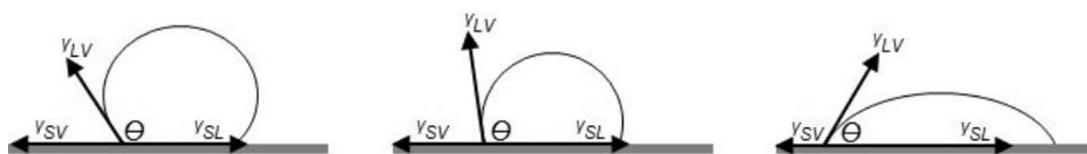
Fig. 6. Contact angle measurements (sessile drop method). The angle, θ, between a drop of liquid on a solid surface and the solid is measured; if water is chosen as the liquid, large angles >90° indicate a hydrophobic surface while angles <90° refer to a hydrophilic surface. The surface tensions or interfacial forces between the materials are given by γ_{SL}, solid/liquid, γ_{LV}, liquid/vapour, and γ_{SV}, solid/vapour.

particle as an inverse image (Villarrubia, 1998) by scanning the probe across a surface containing asperities with a smaller size range than the colloidal probe.

In literature, however, contradicting results can be found. Ooi et al. (2011) concluded that the adhesive forces between model polystyrene carrier particles and micronised salbutamol sulphate particles were unaffected by the diameter of the carrier particles. In contrast, results published by Donovan and Smyth (2010) suggested that the impact of increased carrier size on aerosolisation performance strongly depends on the roughness of the excipient. Larger carrier particles with rougher surfaces enhanced the dispersion performance of a budesonide–lactose blend while the size of smooth lactose particles had to be reduced to improve the dispersibility. The same observation of surface roughness having a more pronounced effect than particle sizes was also noted by others (Kaialy and Nokhodchi, 2013b).

Even though good results can be obtained, the effect of the colloidal probe roughness on the accuracy of the measurements still causes major problems. As discussed in detail by Rabinovich et al. (2002) and Katainen et al. (2006), an uneven surface has a considerable impact on the area of interaction between two bodies in contact making it difficult to calculate the actual contact area. Further inaccuracies occur when the attached drug particles have irregular shapes as the commonly-used models (JKR (Johnson et al., 1971), DMT (Derjaguin et al., 1975)) rely on ideal spheres with well-known diameters. Studies relating morphology to interparticulate forces and formulation performance are therefore not uncommon. While the exact effects of changing morphology can be hard to quantify, researchers agree that decreasing smoothness (which reduces the contact area) leads to decreased adhesive interaction between two bodies and improved formulation performance (Adi et al., 2008, 2013; Götzinger and Peukert, 2003; Hooton et al., 2003).

Beach et al. (2002) evaluated the impact of geometry and roughness on adhesive forces by imprinting the contact surfaces of beclomethasone dipropionate, lactose and a peptide-type material on a fluoropolymer film and evaluating shape and size from the indentation. They were thus able to explain the broad distribution of snap-off values based on differences in contact area. They observed a saw-tooth pattern in the withdrawing force curve which was caused by the AFM probe sequentially detaching from multiple contact points leading to a series of snap-offs. The group also explained the inadequacies of Rabinovich's theory for the prediction of forces between rigid materials.

Hooton et al. (2004) investigated the combined effects of surface geometry and RH on the adhesive forces between both micronised and supercritical fluid-treated salbutamol sulphate particles and substrates consisting of compressed salbutamol sulphate and highly ordered pyrolytic graphite. From their observations, Hooton et al. (2004) demonstrated the deficiencies of the JKR model (Johnson et al., 1971). The group considered three different scenarios ranging from the impact of a single asperity to the investigation of multiple nanoscale asperities. They also evaluated increasing levels of RH. The results highlight the impact of moisture between the asperities and the associated capillary and adhesive forces (Hooton et al., 2004). Lohrmann et al. (2007)

related the results of both experimental setups to the performance of binary blends of salbutamol sulphate with lactose and mannitol respectively, to measure the impact of RH (0–100%) and to compare colloidal probe AFM measurements to the tensile strength method. As expected, the adhesive interactions were found to grow with increasing RH due to increased capillary forces, leading to a decrease in the performance of the formulation. When compared directly, colloidal probe AFM proved to be superior to the tensile strength technique as the distribution of results was considerably narrower. A number of similar colloidal probe experiments carried out by other groups also confirmed the dominance of capillary forces between particles over electrostatic interactions at increasing levels of humidity (Berard et al., 2002a; Tsukada et al., 2004; Young et al., 2003). These experiments were carried out at different RH and with different API and carrier materials. However, increased RH does not always lead to increased interparticulate forces. Young et al. (2004, 2006) observed the expected increase in cohesion for salbutamol sulphate and disodium cromoglycate particles but noticed a decrease in cohesive interaction at higher levels of RH for triamcinolone acetonide. This irregular result may be due to the decay of long-range electrostatic forces at high RH. It was shown (Price et al., 2002) that the significance of capillary forces at a given RH are dependent on the properties of the API. For a budesonide–lactose combination, capillary forces affect the interparticulate forces strongly below 60% RH, while for salbutamol sulphate–lactose blends they only become dominant above 60% RH. Time studies investigating the aging process of binary drug formulations showed that exposure to different RH affects surface morphology, hence also adhesive interactions (Harder et al., 2011).

A colloidal probe and Raman spectroscopy-based differentiation between prevailing interparticulate forces was performed by Rogueda et al. (2011). They found that, in the presence of a model propellant, budesonide–formoterol formulations are governed by vdW forces. Salmeterol xinafoate–fluticasone propionate formulations are, in contrast, governed by a more complex mechanism including non-specified chemical interactions. Previous research on combined salmeterol xinafoate and fluticasone propionate formulations already indicated the presence of interactions depending on the physical and chemical nature of the particles and the media (Michael et al., 2000, 2001; Theophilus et al., 2006). The exact nature of these interactions has not yet been specified.

In terms of surface energetics and the discrimination between polar and dispersive surface energy components, AFM data was successfully correlated with a theoretical surface component approach (SCA) model. The SCA model included the impact of polar components and was based on results from CA and inverse gas chromatography experiments (Traini et al., 2005). Colloidal probe AFM was used to obtain the separation force of two API particles. The experimental results showed the same tendency as the calculated values. A comparison of the actual and the theoretical ratio of adhesive and cohesive forces, although not matching exactly, also indicated a positive relationship. The results strongly recommend the consideration of polar and non-polar interactions in theoretical models (Traini et al., 2005). Additionally, a linear relationship was identified between the theoretical work of adhesion calculated using CA measurements and results from

colloidal probe AFM (Traini et al., 2006) for the interaction of salbutamol sulphate, budesonide, formoterol fumarate dihydrate and different container materials. The adhesive forces correlated with the polar surface free energies of the respective materials.

Colloidal probe AFM has been shown to be a valuable tool for assessing the interaction between API/carrier particles and container materials. The adhesive interactions between APIs/excipients and different container materials have been evaluated and correlated with the performance of the respective formulations. Typical container materials include, but are not limited to, aluminium (Ashayer et al., 2004; Traini et al., 2006), polytetrafluoroethylene (Traini et al., 2006) and steel (Tsukada et al., 2004). Knowledge of these interactions is particularly relevant for processing and storing DPI formulations. For example, the homogeneity of a formulation may be influenced by particle–wall interactions during the mixing process (Zeng et al., 2000). In addition, the performance of the formulation may be further affected by interactions between the powder and the walls of the inhaler device (Wong et al., 2014; Zeng et al., 2000). AFM measurements are also valuable for understanding the prevailing forces in pressurised MDIs. Colloidal probe force measurements can be performed within liquid cells, allowing the impact of propellants such as 2H, 3H decafluoropentane or 2H, 3H perfluoropentane (Ashayer et al., 2004; Bouhroum et al., 2010; Rogueda et al., 2011; Traini et al., 2005, 2007) to be assessed.

The role and impact of stabilising agents have also been investigated by colloidal probe AFM in several research projects. Binary formulations of lactose and vinyl polymer-coated budesonide particles were prepared. The modified formulations were found to have a higher FPF compared to bends containing pure budesonide particles as a result of decreased interparticulate adhesive forces (Buttini et al., 2008). Tuli et al. (2012), however, showed that the presence of polyvinyl acetate residues increased the adhesion between salbutamol sulphate and polycaprolactone model carriers. The group attributed this effect to strong capillary forces. The effect could be minimised by coating the polycaprolactone carrier particles with either magnesium stearate or leucine. The particles were prepared by immersion into magnesium stearate or leucine solutions, respectively, or by dry coating using a hand mixing method (Alway et al., 1996; Tuli et al., 2012

Tuli et al., 2012). Thus, the surface of the model carrier was covered by an additional hydrophobic layer which reduced the adhesion between carrier and API particles. A similar impact was also observed for lactose and beclomethasone dipropionate particles (Young et al., 2002). Recent studies by Islam et al. (2014) demonstrated the use of a salbutamol sulphate-coated model colloidal probe for comparing the adhesion between hydrophilic–hydrophilic and hydrophilic–hydrophobic surfaces. They compared the adhesion of polymer, silica and salbutamol sulphate-coated silica microspheres to spin-coated polymer films. Again, additional layers of magnesium stearate and leucine, spin-coated onto the polymer surface, had an anti-adherent effect.

4.3. Cohesive adhesive balance (CAB)

Begat et al. (2004a) used the colloidal probe technique to measure the CAB within dry powder formulations. CAB measurements, which assess the ratio of the cohesive and adhesive interaction of API and carrier particles, were first introduced by Nanopharm Ltd. (Nanopharm Ltd., 2009). In CAB measurements, the force of cohesion between an API particle and a flat custom-grown API crystal and the force of adhesion between the same API particle and a flat custom-grown carrier crystal are measured. The approach relies on comparing the interactions between an API particle and two flat substrates which excludes the effects of contact area and makes the two measurements directly comparable. A CAB plot of a binary system (Fig. 7) is constructed by plotting the force of cohesion (between probe A and substrate A) against the force of adhesion (between probe A and substrate B).

The plot shows whether a system is dominated by adhesive or cohesive forces which is important for the development of DPI formulations as agglomeration and segregation, and therefore the fluidisation and dispersion properties of the powder, are affected by the CAB ratio (Begat et al., 2004b).

Begat et al. (2004a) made use of the colloid probe technique to observe the CAB ratio in DPI formulations of salbutamol sulphate and budesonide with the carrier material lactose. To reduce the effects of roughness budesonide, salbutamol sulphate and lactose were crystallised by primary nucleation from solution. CAB graphs were used to describe the dominating forces in the drug/carrier
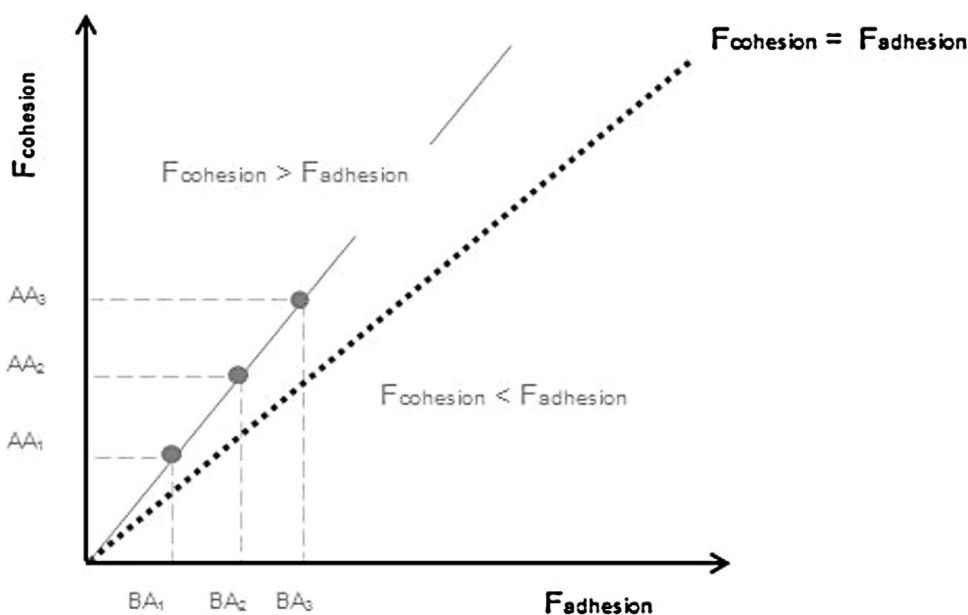

Fig. 7. CAB plot of adhesive against cohesive forces. Three different colloid probes of material A have been used to measure the adhesion between substrate B and A (BA$_1$, BA$_2$, BA$_3$) and the cohesion between substrate A and A (AA$_1$, AA$_2$, AA$_3$). The cohesive forces exceed the adhesive forces.

system and also to demonstrate the capability, reproducibility and applicability of AFM and CAB measurements (Begat et al., 2004a). The CAB technique also served to explain substantial differences in the fluidisation and aerosolisation of poorly and highly cohesive drug particles. The more cohesive particles tended to form agglomerates of increasing size which in turn influences the aerodynamic drag force. Fine particle lactose added as carrier material improved the fluidisation as shown by a shift in the CAB ratio. The study further demonstrated that not only the disaggregation and deposition of the drug itself but also the stability during manufacturing and handling are affected by the CAB ratio within the system (Begat et al., 2004b).

While the CAB approach is useful in many cases (Begat et al., 2005; Hooton et al., 2008, 2006b; Jones et al., 2008a) and is widely used as it overcomes the limitations of instrumental validation and environmental conditions and removes the necessity to normalise the measured force values (Begat et al., 2004a; Nanopharm Ltd., 2009; Traini et al., 2005), it must be remembered that CAB gives a measure of the balance of forces relatively to each other rather than absolute values.

5. Electrical force measurements

High triboelectric charging may lead to severe challenges when performing AFM measurements. Götzinger and Peukert (2003) reported issues regarding the identification of the snap-off force due to the strong attraction between the colloid probe and substrate as a result of high electrostatic charges. It was only after letting the materials rest for two days that the charge had decayed sufficiently to observe the typical snap-off on the force curve.

Triboelectric charging, caused by non-conductive particles colliding with each other or the container, needs to be considered when formulating DPI blends (Zeng et al., 2000). To evaluate electrostatic forces and triboelectric charging, Faraday pails or wells are commonly used (Byron et al., 1997; Elajnaf et al., 2006; Karner and Urbanetz, 2011). Such a device basically consists of two conductive balls or wells of different sizes. The smaller one is placed into the larger, grounded ball/well in a way that prevents their walls from touching. An insulating layer is used to fix the two balls/wells within each other. This construction protects the inner ball/well from unwanted external influences. The electrostatically charged powder is filled into the inner ball/well, leading to an induced charge of the same magnitude on its outer surface. Due to the protecting provided by the outer ball/well, the charge remains constant. The total charge of the powder is then measured by recording the charge between the charged surface of the inner ball/well and the ground with an electrometer. Other techniques for assessment of electrostatic charging include phase Doppler anemometry (Beleca et al., 2010). Such techniques can be also combined with AFM results to gain information about correlations between charging and particulate characteristics. Wong et al. (2014), for example, determined the charge of powdered APIs using a Faraday pail and characterised the surface of the particles through topographical AFM images. Their results showed that a higher degree of crystallinity correlates with increasing consistency of triboelectric charging from container materials. However, these methods only indicate bulk electrostatic charge and are not suitable for evaluating the charge on single particles. Thus, despite that fact that electrostatic charging is generally regarded as a hindrance to AFM measurements, there is also huge potential for developing AFM as a single-particle electrostatic characterisation technique. Bunker et al. (2007) investigated using AFM force curves to assess long-range electrostatic forces at low RH. Snap-in is controlled by the attractive forces between tip and sample and is often dominated by electrostatic forces. Thus, assessment of the surface-tip distance at snap-in enables the relative quantification

of the surface charge on a single particle. Another method was introduced by Kwek et al. (2011). The group set up a parallel plate condenser, included indium tin oxide glass electrodes and positioned a particle at a precisely defined point within the condenser. Recording the force acting on the particle using AFM, they were able to obtain the particle net, induced and image charge.

Even though considerable progress has been made in terms of evaluating electrostatic forces on particulate surface, a commonly applicable method has yet to been found. Only a limited number of researchers have so far contributed to the subject of determining local electric particle properties rather than bulk properties and this area gives room for further developments.

6. Discussion

Looking at the large scope of applications ranging from purely topographical imaging to the determination of interparticulate forces and electrostatic charging, AFM has clearly proved to be one of the most versatile techniques used in pharmaceutical powder research.

Yet throughout the majority of AFM experiments one major issue has become evident: the impact of surface roughness. While the surface texture of a sample is easily accessible by topographical imaging, its actual influence on interparticulate forces is yet far from well-defined. Promising approaches have been made towards modelling the impact of asperities and the determination of contact areas between sample and tip or colloidal probe. SEM imaging and reverse or negative topographical AFM imaging are established methods to assess the area of interaction of a colloidal probe. But even though considerable progress has been made in the area of adhesion measurements, questions still remain over the best method to determine and account for surface roughness, deformation and the actual area of interaction between two bodies. Many researchers have attempted to circumvent these issues by preparing increasingly smooth model particles, thus simplifying analysis considerably. However, this approach usually involves considerable modification of the material surface and it is questionable whether the results are truly representative of real-life situations. Therefore, further improvements are required before colloidal probe AFM can become a reliable mainstream characterisation technique for interparticulate forces. Additionally, AFM settings such as the deflection sensitivity, the applied force, the time of delay between measurements and further parameters have an impact on all results. For this reason, the evaluation of AFM based results should always include a thorough inspection of all details regarding the sample, the probe and the individual settings.

In addition, however useful AFM may be, the technique has its limitations when it comes to the evaluation of a formulation as a whole. Particle properties are only recorded for individual particles and bulk properties of the formulation are not measured. Also, single particles are scanned in an isolated environment and possible effects from tightly adjoined particles are neglected. Even colloidal probe measurements only give an idea of the forces between two particles, again under isolated and exemplary conditions. To give just a few examples, any movements within a formulation; the influence of permanent friction; and the impact of particles pressing onto each other are excluded.

7. Conclusions

AFM in general offers a wide range of possibilities for determining the material, surface and formulation characteristics within dry powder blends (Shur and Price, 2012). Some techniques, such as the evaluation of surface morphology, are already firmly established within pharmaceutical research while others, in

particular colloidal probe AFM, have gained significantly in importance over the last decade.

Increased interest in AFM as a characterisation technique, along with the production of more accessible instruments with a range of novel analysis modes has led to new, innovative approaches to materials characterisation such as the assessment of rheological properties (Crean et al., 2009) and the incorporation of a condenser (Kwek et al., 2011) to determine particle charges via AFM. Referring back to the review of AFM adhesion measurements of interparticulate forces by Roberts (2005), much progress has been made in the last decade. The constant improvement in instrumentation, along with the development of a wide range of novel applications, has made AFM-based techniques significant for the characterisation of pharmaceutical materials, and especially important for applications such as DPI formulations.

With further refinements, especially in terms of adhesion measurements, AFM will certainly become even more important to pre-evaluate the performance of inhalation formulations. Considering the constantly improving colloidal probe technique, AFM seems to offer one of the most straightforward methods to reliably compare the adhesion between differently processed particles and therefore also to quickly eliminate poorly performing components. The possibility of directly linking surface properties and interparticulate forces may be the largest advantage in this regard.

Acknowledgements

References

Adi, H., Larson, I., Stewart, P.J., 2007. Adhesion and redistribution of salmeterol xinafoate particles in sugar-based mixtures for inhalation. Int. J. Pharm. 337, 229–238.

Adi, H., Traini, D., Chan, H.K., Young, P.M., 2008. The influence of drug morphology on aerosolisation efficiency of dry powder inhaler formulations. J. Pharm. Sci. 97, 2780–2788.

Adi, S., Adi, H., Chan, H.-K., Tong, Z., Yang, R., Yu, A., 2013. Effects of mechanical impaction on aerosol performance of particles with different surface roughness. Powder Technol. 236, 164–170.

Ashayer, R., Luckham, P.F., Manimaaran, S., Rogueda, P., 2004. Investigation of the molecular interactions in a pMDI formulation by atomic force microscopy. Eur. J. Pharm. Sci. 21, 533–543.

Bassam, F., York, P., Rowe, R., Roberts, R., 1990. Young's modulus of powders used as pharmaceutical excipients. Int. J. Pharm. 64, 55–60.

Beach, E., Tormoen, G., Drelich, J., Han, R., 2002. Pull-off force measurements between rough surfaces by atomic force microscopy. J. Colloid Interf. Sci. 247, 84–99.

Begat, P., Morton, D.A., Staniforth, J.N., Price, R., 2004a. The cohesive–adhesive balances in dry powder inhaler formulations I: direct quantification by atomic force microscopy. Pharm. Res. 21, 1591–1597.

Begat, P., Morton, D.A., Staniforth, J.N., Price, R., 2004b. The cohesive–adhesive balances in dry powder inhaler formulations II: Influence on fine particle delivery characteristics. Pharm. Res. 21, 1826–1833.

Begat, P., Price, R., Harris, H., Morton, D.A., Staniforth, J.N., 2005. The influence of force control agents on the cohesive–adhesive balance in dry powder inhaler formulations. KONA Powder Part. J. 23, 109–121.

Begat, P., Young, P.M., Edge, S., Kaerger, J.S., Price, R., 2003. The effect of mechanical processing on surface stability of pharmaceutical powders: visualization by atomic force microscopy. J. Pharm. Sci. 92, 611–620.

Beilmann, B., Kubiak, R., Grab, P., Häusler, H., Langguth, P., 2007. Effect of interactive ternary mixtures on dispersion characteristics of ipratropium bromide in dry powder inhaler formulations. AAPS PharmSciTech 8, E32–E39.

Beleca, R., Abbod, M., Balachandran, W., Miller, P.R., 2010. Investigation of electrostatic properties of pharmaceutical powders using phase Doppler anemometry. IEEE Trans. Ind. Appl. 46, 1181–1187.

Benmouna, F., Johannsmann, D., 2003. Hydrodynamics of particle–wall interaction in colloidal probe experiments: comparison of vertical and lateral motion. J. Phys. Condens. Matter 15, 3003–3012.

Berard, V., Lesniewska, E., Andres, C., Pertuy, D., Laroche, C., Pourcelot, Y., 2002a. Affinity scale between a carrier and a drug in DPI studied by atomic force microscopy. Int. J. Pharm. 247, 127–137.

Berard, V., Lesniewska, E., Andres, C., Pertuy, D., Laroche, C., Pourcelot, Y., 2002b. Dry powder inhaler: influence of humidity on topology and adhesion studied by AFM. Int. J. Pharm. 232, 213–224.

Bhushan, B., 2003. Adhesion and stiction: mechanisms, measurement techniques, and methods for reduction. J. Vac. Sci. Technol. B 21, 2262–2296.

Bhushan, B., 2010. Handbook of Micro/nano Tribology. CRC Press.

Binnig, G., Gerber, C., Stoll, E., Albrecht, T., Quate, C., 1987. Atomic resolution with atomic force microscope. EPL (Europhys. Lett.) 3, 1281–1283.

Binnig, G., Quate, C.F., Gerber, C., 1986. Atomic force microscope. Phys. Rev. Lett. 56, 930–934.

Binnig, G., Rohrer, H., 1981. Raster-Kraftmikroskop, Patent CH000000643397A, IBM Corp., Switzerland.

Bosquillon, C., Lombry, C., Preat, V., Vanbever, R., 2001. Influence of formulation excipients and physical characteristics of inhalation dry powders on their aerosolization performance. J. Control. Release 70, 329–339.

Bouhroum, A., Burley, J.C., Champness, N.R., Toon, R.C., Jinks, P.A., Williams, P.M., Roberts, C.J., 2010. An assessment of beclomethasone dipropionate clathrate formation in a model suspension metered dose inhaler. Int. J. Pharm. 391, 98–106.

Bunker, M.J., Davies, M.C., James, M.B., Roberts, C.J., 2007. Direct observation of single particle electrostatic charging by atomic force microscopy. Pharm. Res. 24, 1165–1169.

Butt, H.-J., 1991. Measuring electrostatic, van der Waals, and hydration forces in electrolyte solutions with an atomic force microscope. Biophys. J. 60, 1438–1444.

Butt, H.-J., Cappella, B., Kappl, M., 2005. Force measurements with the atomic force microscope: technique, interpretation and applications. Surf. Sci. Rep. 59, 1–152.

Buttini, F., Colombo, P., Wenger, M., Mesquida, P., Marriott, C., Jones, S.A., 2008. Back to basics: the development of a simple, homogenous, two-component dry-powder inhaler formulation for the delivery of budesonide using miscible vinyl polymers. J. Pharm. Sci. 97, 1257–1267.

Byron, P.R., Peart, J., Staniforth, J.N., 1997. Aerosol electrostatics I: properties of fine powders before and after aerosolization by dry powder inhalers. Pharm. Res. 14, 698–705.

Cappella, B., Dietler, G., 1999. Force-distance curves by atomic force microscopy. Surf. Sci. Rep. 34, 1–104.

Chan, H.-K., 2008. What is the role of particle morphology in pharmaceutical powder aerosols? Expert Opin. Drug Deliv. 5, 909–914.

Chow, A.H., Tong, H.H., Chattopadhyay, P., Shekunov, B.Y., 2007. Particle engineering for pulmonary drug delivery. Pharm. Res. 24, 411–437.

Chrystyn, H., Price, D., 2009. Not all asthma inhalers are the same: factors to consider when prescribing an inhaler. Prim. Care Respir. J. 18, 243–249.

Cleveland, J., Manne, S., Bocek, D., Hansma, P., 1993. A nondestructive method for determining the spring constant of cantilevers for scanning force microscopy. Rev. Sci. Instrum. 64, 403–405.

Cline, D., Dalby, R., 2002. Predicting the quality of powders for inhalation from surface energy and area. Pharm. Res. 19, 1274–1277.

Craig, V.S., Neto, C., 2001. In situ calibration of colloid probe cantilevers in force microscopy: hydrodynamic drag on a sphere approaching a wall. Langmuir 17, 6018–6022.

Crean, B., Chen, X., Banks, S.R., Cook, W.G., Melia, C.D., Roberts, C.J., 2009. An investigation into the rheology of pharmaceutical inter-granular material bridges at high shear rates. Pharm. Res. 26, 1101–1111.

Cui, Y., Schmalfuß, S., Zellnitz, S., Sommerfeld, M., Urbanetz, N., 2014. Towards the optimisation and adaptation of dry powder inhalers. Int. J. Pharm. 470, 120–132.

Cui, Y., Sommerfeld, M., 2015. Forces on micron-sized particles randomly distributed on the surface of larger particles and possibility of detachment. Int. J. Multiphase Flow 72, 39–52.

Dalby, R., Spallek, M., Voshaar, T., 2004. A review of the development of Respimat® Soft Mist™ Inhaler. Int. J. Pharm. 283, 1–9.

Danesh, A., Chen, X., Davies, M., Roberts, C., Sanders, G., Tendler, S., Williams, P., Wilkins, M., 2000. Polymorphic discrimination using atomic force microscopy: distinguishing between two polymorphs of the drug cimetidine. Langmuir 16, 866–870.

Davies, M., Brindley, A., Chen, X., Marlow, M., Doughty, S.W., Shrubb, I., Roberts, C.J., 2005. Characterization of drug particle surface energetics and Young's modulus by atomic force microscopy and inverse gas chromatography. Pharm. Res. 22, 1158–1166.

De Boer, A., Hagedoorn, P., Gjaltema, D., Goede, J., Frijlink, H., 2003a. Air classifier technology (ACT) in dry powder inhalation: Part 1. Introduction of a novel force distribution concept (FDC) explaining the performance of a basic air classifier on adhesive mixtures. Int. J. Pharm. 260, 187–200.

De Boer, A., Hagedoorn, P., Gjaltema, D., Goede, J., Kussendrager, K., Frijlink, H., 2003b. Air classifier technology (ACT) in dry powder inhalation Part 2. The effect of lactose carrier surface properties on the drug-to-carrier interaction in adhesive mixtures for inhalation. Int. J. Pharm. 260, 201–216.

De Boer, A., Dickhoff, B., Hagedoorn, P., Gjaltema, D., Goede, J., Lambregts, D., Frijlink, H., 2005. A critical evaluation of the relevant parameters for drug redispersion from adhesive mixtures during inhalation. Int. J. Pharm. 294, 173–184.

Derjaguin, B., Muller, V., Toporov, Y.P., 1975. Effect of contact deformations on the adhesion of particles. J. Colloid Interf. Sci. 53, 314–326.

Donovan, M.J., Smyth, H.D., 2010. Influence of size and surface roughness of large lactose carrier particles in dry powder inhaler formulations. Int. J. Pharm. 402, 1–9.

Dos Santos Ferreira, O., Gelinck, E., de Graaf, D., Fischer, H., 2010. Adhesion experiments using an AFM—parameters of influence. Appl. Surf. Sci. 257, 48–55.

Deutsches Patent-und Markenamt, 2014. Erfindergalerie des DPMA: Prof. Gerd BinnigDPMA, Munich, Germany. . (accessed 11.05.14.) http://www.dpma.de/ponline/erfindergalerie/e_bio_binnig.html.

Ducker, W.A., Senden, T.J., Pashley, R.M., 1991. Direct measurement of colloidal forces using an atomic force microscope. Nature 353, 239–241.

Durbin, S.D., Carlson, W.E., 1992. Lysozyme crystal growth studied by atomic force microscopy. J. Cryst. Growth 122, 71–79.

Eaton, P.J., West, P., 2010. Atomic Force Microscopy. Oxford University Press, Oxford.

Egart, M., Ilić, I., Janković, B., Lah, N., Srčič, S., 2014. Compaction properties of crystalline pharmaceutical ingredients according to the Walker model and nanomechanical attributes. Int. J. Pharm. 472, 347–355.

Elajnaf, A., Carter, P., Rowley, G., 2006. Electrostatic characterisation of inhaled powders: effect of contact surface and relative humidity. Eur. J. Pharm. Sci. 29, 375–384.

Eve, J., Patel, N., Luk, S., Ebbens, S., Roberts, C., 2002. A study of single drug particle adhesion interactions using atomic force microscopy. Int. J. Pharm. 238, 17–27.

Ferrari, F., Cocconi, D., Bettini, R., Giordano, F., Santi, P., Tobyn, M., Price, R., Young, P., Caramella, C., Colombo, P., 2004. The surface roughness of lactose particles can be modulated by wet-smoothing using a high-shear mixer. AAPS Pharmscitech 5, 69–74.

Flament, M.-P., Leterme, P., Gayot, A., 2004. The influence of carrier roughness on adhesion, content uniformity and the in vitro deposition of terbutaline sulphate from dry powder inhalers. Int. J. Pharm. 275, 201–209.

Frijlink, H., De Boer, A., 2004. Dry powder inhalers for pulmonary drug delivery. Expert Opin. Drug Deliv. 1, 67–86.

Fröberg, J., Rojas, O., Claesson, P., 1999. Surface forces and measuring techniques. Int. J. Miner. Process. 56, 1–30.

Gates, R.S., Reitsma, M.G., 2007. Precise atomic force microscope cantilever spring constant calibration using a reference cantilever array. Rev. Sci. Instrum. 78, 86101.

Genina, N., Räikkönen, H., Heinämäki, J., Antikainen, O., Siiriä, S., Veski, P., Yliruusi, J., 2009. Effective modification of particle surface properties using ultrasonic water mist. AAPS PharmSciTech 10, 282–288.

Giessibl, F.J., 2005. AFM's path to atomic resolution. Mater. Today 8, 32–41.

Global Initiative for Asthma, 2014. Pocket Guide for Asthma Management and PreventionGINA. . (accessed 06.01.15.) http://www.ginasthma.org/documents/1.

Glotzbach, C., Stephan, D., Schmidt, M., 2013. Measuring interparticle forces: evaluation of superplasticizers for microsilica via colloidal probe technique. Cem. Concr. Compos. 36, 42–47.

Götzinger, M., Peukert, W., 2003. Dispersive forces of particle–surface interactions: direct AFM measurements and modelling. Powder Technol. 130, 102–109.

Green, C.P., Lioe, H., Cleveland, J.P., Proksch, R., Mulvaney, P., Sader, J.E., 2004. Normal and torsional spring constants of atomic force microscope cantilevers. Rev. Sci. Instrum. 75, 1988–1996.

Guenette, E., Barrett, A., Kraus, D., Brody, R., Harding, L., Magee, G., 2009. Understanding the effect of lactose particle size on the properties of DPI formulations using experimental design. Int. J. Pharm. 380, 80–88.

Harder, C., Lesniewska, E., Laroche, C., 2011. Study of ageing of dry powder inhaler and metered dose inhaler by atomic force microscopy. Powder Technol. 208, 252–259.

Harkins, W., 1928. Surface energy and the orientation of molecules in surfaces as revealed by surface energy relations. Zeitschrift für Physikalische Chemie 139, 647–691.

Healy, A.M., Amaro, M.I., Paluch, K.J., Tajber, L., 2014. Dry powders for oral inhalation free of lactose carrier particles. Adv. Drug Deliv. Rev. 7, 32–52.

Heng, P.W.S., Wah, L., Theng, L., 2000. Quantification of the surface morphologies of lactose carriers and their efl'ect on the in vitro deposition of salbutamol sulphate. Chem. Pharm. Bull. 48, 393.

Hertz, H., 1882. Ueber die Berührung fester elastischer Körper. Journal für die reine und angewandte Mathematik 92, 156–171.

Heyder, J., 2004. Deposition of inhaled particles in the human respiratory tract and consequences for regional targeting in respiratory drug delivery. Proc. Am. Thorac. Soc. 1, 315–320.

Hickey, A.J., Mansour, H.M., Telko, M.J., Xu, Z., Smyth, H.D., Mulder, T., McLean, R., Langridge, J., Papadopoulos, D., 2007. Physical characterization of component particles included in dry powder inhalers. I. Strategy review and static characteristics. J. Pharm. Sci. 96, 1282–1301.

Hooton, J.C., German, C.S., Allen, S., Davies, M.C., Roberts, C.J., Tendler, S.J., Williams, P.M., 2003. Characterization of particle-interactions by atomic force microscopy: effect of contact area. Pharm. Res. 20, 508–514.

Hooton, J.C., German, C.S., Allen, S., Davies, M.C., Roberts, C.J., Tendler, S.J., Williams, P.M., 2004. An atomic force microscopy study of the effect of nanoscale contact geometry and surface chemistry on the adhesion of pharmaceutical particles. Pharm. Res. 21, 953–961.

Hooton, J.C., German, C.S., Davies, M.C., Roberts, C.J., 2006a. A comparison of morphology and surface energy characteristics of sulfathiazole polymorphs based upon single particle studies. Eur. J. Pharm. Sci. 28, 315–324.

Hooton, J.C., Jones, M.D., Price, R., 2006b. Predicting the behavior of novel sugar carriers for dry powder inhaler formulations via the use of a cohesive–adhesive force balance approach. J. Pharm. Sci. 95, 1288–1297.

Hooton, J.C., Jones, M.D., Harris, H., Shur, J., Price, R., 2008. The influence of crystal habit on the prediction of dry powder inhalation formulation performance using the cohesive–adhesive force balance approach. Drug Dev. Ind. Pharm. 34, 974–983.

Hoppentocht, M., Hagedoorn, P., Frijlink, H.W., de Boer, A.H., 2014. Technological and practical challenges of dry powder inhalers and formulations. Adv. Drug Deliv. Rev. 75, 18–31.

Hutter, J.L., Bechhoefer, J., 1993a. Calibration of atomic-force microscope tips. Rev. Sci. Instrum. 64, 1868–1873.

Hutter, J.L., Bechhoefer, J., 1993b. Manipulation of van der Waals forces to improve image resolution in atomic-force microscopy. J. Appl. Phys. 73, 4123–4129.

Islam, N., Tuli, R.A., George, G.A., Dargaville, T.R., 2014. Colloidal drug probe: method development and validation for adhesion force measurement using atomic force microscopy. Adv. Powder Technol. 25, 1240–1248.

Israelachvili, J.N., 2011. Intermolecular and Surface Forces: Revised Third Edition. Academic Press.

James, J., Crean, B., Davies, M., Toon, R., Jinks, P., Roberts, C.J., 2008. The surface characterisation and comparison of two potential sub-micron, sugar bulking excipients for use in low-dose, suspension formulations in metered dose inhalers. Int. J. Pharm. 361, 209–221.

Johnson, K., Kendall, K., Roberts, A., 1971. Surface energy and the contact of elastic solids. Proceedings of the Royal Society of London. A. Mathematical and Physical Sciences 324, 301–313.

Jones, M.D., Harris, H., Hooton, J.C., Shur, J., King, G.S., Mathoulin, C.A., Nichol, K., Smith, T.L., Dawson, M.L., Ferrie, A.R., 2008a. An investigation into the relationship between carrier-based dry powder inhalation performance and formulation cohesive–adhesive force balances. Eur. J. Pharm. Biopharm. 69, 496–507.

Jones, M.D., Hooton, J.C., Dawson, M.L., Ferrie, A.R., Price, R., 2008b. An investigation into the dispersion mechanisms of ternary dry powder inhaler formulations by the quantification of interparticulate forces. Pharm. Res. 25, 337–348.

Jones, M.D., Price, R., 2006. The influence of fine excipient particles on the performance of carrier-based dry powder inhalation formulations. Pharm. Res. 23, 1665–1674.

Kaialy, W., Martin, G.P., Ticehurst, M.D., Royall, P., Mohammad, M.A., Murphy, J., Nokhodchi, A., 2011. Characterisation and deposition studies of recrystallised lactose from binary mixtures of ethanol/butanol for improved drug delivery from dry powder inhalers. AAPS J. 13, 30–43.

Kaialy, W., Momin, M.N., Ticehurst, M.D., Murphy, J., Nokhodchi, A., 2010. Engineered mannitol as an alternative carrier to enhance deep lung penetration of salbutamol sulphate from dry powder inhaler. Colloids Surf. B Biointerf. 79, 345–356.

Kaialy, W., Nokhodchi, A., 2012. Antisolvent crystallisation is a potential technique to prepare engineered lactose with promising aerosolisation properties: effect of saturation degree. Int. J. Pharm. 437, 57–69.

Kaialy, W., Nokhodchi, A., 2013a. Freeze-dried mannitol for superior pulmonary drug delivery via dry powder inhaler. Pharm. Res. 30, 458–477.

Kaialy, W., Nokhodchi, A., 2013b. Treating mannitol in a saturated solution of mannitol: a novel approach to modify mannitol crystals for improved drug delivery to the lungs. Int. J. Pharm. 448, 58–70.

Karner, S., Maier, M., Littringer, E., Urbanetz, N.A., 2014. Surface roughness effects on the tribo-charging and mixing homogeneity of adhesive mixtures used in dry powder inhalers. Powder Technol. 264, 544–549.

Karner, S., Urbanetz, N.A., 2011. The impact of electrostatic charge in pharmaceutical powders with specific focus on inhalation-powders. J. Aerosol Sci. 42, 428–445.

Katainen, J., Paajanen, M., Ahtola, E., Pore, V., Lahtinen, J., 2006. Adhesion as an interplay between particle size and surface roughness. J. Colloid Interf. Sci. 304, 524–529.

Kinnunen, H., Hebbink, G., Peters, H., Shur, J., Price, R., 2014. Defining the critical material attributes of lactose monohydrate in carrier based dry powder inhaler formulations using artificial neural networks. AAPS PharmSciTech 15, 1009–1020.

Kubavat, H.A., Shur, J., Ruecroft, G., Hipkiss, D., Price, R., 2012. Influence of primary crystallisation conditions on the mechanical and interfacial properties of micronised budesonide for dry powder inhalation. Int. J. Pharm. 430, 26–33.

Kwek, J.W., Vakarelski, I.U., Ng, W.K., Heng, J.Y., Tan, R.B., 2011. Novel parallel plate condenser for single particle electrostatic force measurements in atomic force microscope. Colloid Surf. A-Physicochem. Eng. Asp. 385, 206–212.

Labiris, N., Dolovich, M., 2003a. Pulmonary drug delivery. Part I: physiological factors affecting therapeutic effectiveness of aerosolized medications. Br. J. Clin. Pharmacol. 56, 588–599.

Labiris, N.R., Dolovich, M.B., 2003b. Pulmonary drug delivery. Part II: the role of inhalant delivery devices and drug formulations in therapeutic effectiveness of aerosolized medications. Br. J. Clin. Pharmacol. 56, 600–612.

Lam, K.K., Newton, J.M., 1991. Investigation of applied compression on the adhesion of powders to a substrate surface. Powder Technol. 65, 167–175.

Lamprou, D., Smith, J.R., 2014. Applications of AFM in pharmaceutical sciences. In: Rades, T., Mullertz, A., Perrie, Y. (Eds.), Analytical Techniques in Pharmaceutical Sciences. Springer.

Leite, F.L., Bueno, C.C., Da Róz, A.L., Ziemath, E.C., Oliveira, O.N., 2012. Theoretical models for surface forces and adhesion and their measurement using atomic force microscopy. Int. J. Mol. Sci. 13, 12773–12856.

Lohrmann, M., Kappl, M., Butt, H.-J., Urbanetz, N.A., Lippold, B.C., 2007. Adhesion forces in interactive mixtures for dry powder inhalers—evaluation of a new measuring method. Eur. J. Pharm. Biopharm. 67, 579–586.

Louey, M.D., Mulvaney, P., Stewart, P.J., 2001. Characterisation of adhesional properties of lactose carriers using atomic force microscopy. J. Pharm. Biom. Anal. 25, 559–567.

Masterson, V.M., Cao, X., 2008. Evaluating particle hardness of pharmaceutical solids using AFM nanoindentation. Int. J. Pharm. 362, 163–171.

Michael, Y., Chowdhry, B.Z., Ashurst, I.C., Snowden, M.J., Davies-Cutting, C., Gray, S., 2000. The physico-chemical properties of salmeterol and fluticasone propionate in different solvent environments. Int. J. Pharm. 200, 279–288.

Michael, Y., Snowden, M.J., Chowdhry, B.Z., Ashurst, I.C., Davies-Cutting, C.J., Riley, T., 2001. Characterisation of the aggregation behaviour in a salmeterol and fluticasone propionate inhalation aerosol system. Int. J. Pharm. 221, 165–174.

Muller, V., Yushchenko, V., Derjaguin, B., 1980. On the influence of molecular forces on the deformation of an elastic sphere and its sticking to a rigid plane. J. Colloid Interf. Sci. 77, 91–101.

Nanopharm Ltd, 2009. Cohesive-Adhesive Balance (CAB)Nanopharm Ltd.. . (accessed 06.12.14.) http://www.nanopharm.co.uk/Technology_Cohesive-Adhesive-Balance.php.

Neumann, B., 1967. The flow properties of powders. Adv. Pharm. Sci. 2, 191–221.

Notley, S.M., Biggs, S., Craig, V.S., 2003. Calibration of colloid probe cantilevers using the dynamic viscous response of a confined liquid. Rev. Sci. Instrum. 74, 4026–4032.

Ohler, B., 2007. Practical Advice on the Determination of Cantilever Spring Constants. Application Note An94. Veeco Instruments Inc..

Onuma, K., Ito, A., Tateishi, T., Kameyama, T., 1995. Surface observations of synthetic hydroxyapatite single crystal by atomic force microscopy. J. Cryst. Growth 148, 201–206.

Ooi, J., Traini, D., Hoe, S., Wong, W., Young, P.M., 2011. Does carrier size matter? A fundamental study of drug aerosolisation from carrier based dry powder inhalation systems. Int. J. Pharm. 413, 1–9.

Packhaeuser, C.B., Lahnstein, K., Sitterberg, J., Schmehl, T., Gessler, T., Bakowsky, U., Seeger, W., Kissel, T., 2009. Stabilization of aerosolizable nano-carriers by freeze-drying. Pharm. Res. 26, 129–138.

Paranjpe, M., Müller-Goymann, C.C., 2014. Nanoparticle-mediated pulmonary drug delivery: a review. Int. J. Mol. Sci. 15, 5852–5873.

Parkin, J.D., Hähner, G., 2013. Determination of the spring constants of the higher flexural modes of microcantilever sensors. Nanotechnology 24, 65704.

Parkin, J.D., Hähner, G., 2014. Calibration of the torsional and lateral spring constants of cantilever sensors. Nanotechnology 25, 225701.

Patton, J.S., Byron, P.R., 2007. Inhaling medicines: delivering drugs to the body through the lungs. Nat. Rev. Drug Discov. 6, 67–74.

Perkins, M., Bunker, M., James, J., Rigby-Singleton, S., Ledru, J., Madden-Smith, C., Luk, S., Patel, N., Roberts, C., 2009. Towards the understanding and prediction of material changes during micronisation using atomic force microscopy. Eur. J. Pharm. Sci. 38 (1), 1–8.

Perkins, M., Ebbens, S.J., Hayes, S., Roberts, C.J., Madden, C.E., Luk, S.Y., Patel, N., 2007. Elastic modulus measurements from individual lactose particles using atomic force microscopy. Int. J. Pharm. 332, 168–175.

Pittenger, B., Erina, N., Su, C., 2010. Quantitative Mechanical Property Mapping at the Nanoscale with Peakforce Qnm. Application Note An128. Veeco Instruments Inc..

Podczeck, F., Newton, J.M., James, M.B., 1994. Assessment of adhesion and autoadhesion forces between particles and surfaces. J. Adhes. Sci. Technol. 8, 1459–1472.

Podczeck, F., Newton, J.M., James, M.B., 1997. Influence of relative humidity of storage air on the adhesion and autoadhesion of micronized particles to particulate and compacted powder surfaces. J. Colloid Interf. Sci. 187, 484–491.

Price, R., Young, P., Edge, S., Staniforth, J., 2002. The influence of relative humidity on particulate interactions in carrier-based dry powder inhaler formulations. Int. J. Pharm. 246, 47–59.

Price, R., Young, P.M., 2004. Visualization of the crystallization of lactose from the amorphous state. J. Pharm. Sci. 93, 155–164.

Rabinovich, Y.I., Adler, J.J., Ata, A., Singh, R.K., Moudgil, B.M., 2000a. Adhesion between nanoscale rough surfaces: I. Role of asperity geometry. J. Colloid Interf. Sci. 232, 10–16.

Rabinovich, Y.I., Adler, J.J., Ata, A., Singh, R.K., Moudgil, B.M., 2000b. Adhesion between nanoscale rough surfaces: II. Measurement and comparison with theory. J. Colloid Interf. Sci. 232, 17–24.

Rabinovich, Y.I., Adler, J.J., Esayanur, M.S., Ata, A., Singh, R.K., Moudgil, B.M., 2002. Capillary forces between surfaces with nanoscale roughness. Adv. Colloid Interf. Sci. 96, 213–230.

Roberts, C.J., 2005. What can we learn from atomic force microscopy adhesion measurements with single drug particles? Eur. J. Pharm. Sci. 24, 153–157.

Rogueda, P.G., Price, R., Smith, T., Young, P.M., Traini, D., 2011. Particle synergy and aerosol performance in non-aqueous liquid of two combinations metered dose inhalation formulations: an AFM and Raman investigation. J. Colloid Interf. Sci. 361, 649–655.

Sader, J.E., Chon, J.W., Mulvaney, P., 1999. Calibration of rectangular atomic force microscope cantilevers. Rev. Sci. Instrum. 70, 3967–3969.

Sader, J.E., Larson, I., Mulvaney, P., White, L.R., 1995. Method for the calibration of atomic force microscope cantilevers. Rev. Sci. Instrum. 66, 3789–3798.

Schmaltz, G., 1929. Über Glätte und Ebenheit als physikalisches und physiologisches problem. Zeitschrift des Vereines deutcher Ingenieure 73, 1461–1467.

Serry, F., 2005. Improving the Accuracy of Afm Force Measurements: The Thermal Tune Solution to the Cantilever Spring Constant Problem. Application Notes 1–4. Veeco Instruments Inc..

Shur, J., Kubavat, H.A., Ruecroft, G., Hipkiss, D., Price, R., 2012. Influence of crystal form of ipratropium bromide on micronisation and aerosolisation behaviour in dry powder inhaler formulations. J. Pharm. Pharmacol. 64, 1326–1336.

Shur, J., Price, R., 2012. Advanced microscopy techniques to assess solid-state properties of inhalation medicines. Adv. Drug Deliv. Rev. 64, 369–382.

Sindel, U., Zimmermann, I., 2001. Measurement of interaction forces between individual powder particles using an atomic force microscope. Powder Technol. 117, 247–254.

Sung, J.C., Pulliam, B.L., Edwards, D.A., 2007. Nanoparticles for drug delivery to the lungs. Trends Biotechnol. 25, 563–570.

Tabor, D., 1977. Surface forces and surface interactions. J. Colloid Interf. Sci. 58, 2–13.

Tan, S., Newton, J., 1990. Powder flowability as an indication of capsule filling performance. Int. J. Pharm. 61, 145–155.

Theophilus, A., Moore, A., Prime, D., Rossomanno, S., Whitcher, B., Chrystyn, H., 2006. Co-deposition of salmeterol and fluticasone propionate by a combination inhaler. Int. J. Pharm. 313, 14–22.

Thompson, C., Davies, M.C., Roberts, C.J., Tendler, S.J., Wilkinson, M.J., 2004. The effects of additives on the growth and morphology of paracetamol (acetaminophen) crystals. Int. J. Pharm. 280, 137–150.

Traini, D., Rogueda, P., Young, P., Price, R., 2005. Surface energy and interparticle force correlation in model pMDI formulations. Pharm. Res. 22, 816–825.

Traini, D., Young, P.M., Rogueda, P., Price, R., 2006. The use of AFM and surface energy measurements to investigate drug–canister material interactions in a model pressurized metered dose inhaler formulation. Aerosol Sci. Technol. 40, 227–236.

Traini, D., Young, P.M., Rogueda, P., Price, R., 2007. In vitro investigation of drug particulates interactions and aerosol performance of pressurised metered dose inhalers. Pharm. Res. 24, 125–135.

Tsukada, M., Irie, R., Yonemochi, Y., Noda, R., Kamiya, H., Watanabe, W., Kauppinen, E., 2004. Adhesion force measurement of a DPI size pharmaceutical particle by colloid probe atomic force microscopy. Powder Technol. 141, 262–269.

Tuli, R.A., Dargaville, T.R., George, G.A., Islam, N., 2012. Polycaprolactone microspheres as carriers for dry powder inhalers: effect of surface coating on aerosolization of salbutamol sulfate. J. Pharm. Sci. 101, 733–745.

Villarrubia, J.S., 1998. Strategy for faster blind reconstruction of tip geometry for scanned probe microscopy. 23rd Annual International Symposium on Microlithography. International Society for Optics and Photonics 10–18.

Wang, Y.-B., Watts, A.B., Peters, J.I., Williams III, R.O., 2014. The impact of pulmonary diseases on the fate of inhaled medicines—a review. Int. J. Pharm. 461, 112–128.

Ward, S., Perkins, M., Zhang, J., Roberts, C.J., Madden, C.E., Luk, S.Y., Patel, N., Ebbens, S.J., 2005. Identifying and mapping surface amorphous domains. Pharm. Res. 22, 1195–1202.

Wong, J., Kwok, P.C.L., Noakes, T., Fathi, A., Dehghani, F., Chan, H.-K., 2014. Effect of crystallinity on electrostatic charging in dry powder inhaler formulations. Pharm. Res. 31, 1656–1664.

Wu, X., Li, X., Mansour, H.M., 2010. Surface analytical techniques in solid-state particle characterization for predicting performance in dry powder inhalers. KONA Powder Part. J. 28, 3–19.

Yip, C.M., Ward, M.D., 1996. Atomic force microscopy of insulin single crystals: direct visualization of molecules and crystal growth. Biophys. J. 71, 1071–1078.

Young, P.M., Kwok, P., Adi, H., Chan, H.-K., Traini, D., 2009. Lactose composite carriers for respiratory delivery. Pharm. Res. 26, 802–810.

Young, P.M., Price, R., Tobyn, M.J., Buttrum, M., Dey, F., 2003. Investigation into the effect of humidity on drug–drug interactions using the atomic force microscope. J. Pharm. Sci. 92, 815–822.

Young, P.M., Price, R., Tobyn, M.J., Buttrum, M., Dey, F., 2004. The influence of relative humidity on the cohesion properties of micronized drugs used in inhalation therapy. J. Pharm. Sci. 93, 753–761.

Young, P.M., Tobyn, M.J., Price, R., Buttrum, M., Dey, F., 2006. The use of colloid probe microscopy to predict aerosolization performance in dry powder inhalers: AFM and in vitro correlation. J. Pharm. Sci. 95, 1800–1809.

Young, R., Ward, J., Scire, F., 1972. The topografiner: an instrument for measuring surface microtopography. Rev. Sci. Instrum. 43, 999–1011.

Young, T., 1805. An essay on the cohesion of fluids. Philos. Trans. R. Soc. Lond. 65–87.

Zellnitz, S., Redlinger-Pohn, J.D., Kappl, M., Schroettner, H., Urbanetz, N.A., 2013. Preparation and characterization of physically modified glass beads used as model carriers in dry powder inhalers. Int. J. Pharm. 447, 132–138.

Zellnitz, S., Schroettner, H., Urbanetz, N.A., 2014. Surface modified glass beads as model carriers in dry powder inhalers—influence of drug load on the fine particle fraction. Powder Technol. 268, 377–386.

Zeng, X.M., Martin, G.P., Marriott, C., 2000. Particulate Interactions in Dry Powder Formulation for Inhalation. Taylor & Francis.

Zhang, J., Wu, L., Chan, H.-K., Watanabe, W., 2011. Formation, characterization, and fate of inhaled drug nanoparticles. Adv. Drug Deliv. Rev. 63, 441–455.